

Design, Synthesis, and Biological Evaluation of Novel
Pyrimido[4,5-*b*]indole Derivatives Against Gram-Negative
Multidrug-Resistant PathogensQidi Kong, Wei Pan, Heng Xu, Yaru Xue, Bin Guo, Xin Meng, Cheng Luo, Ting Wang, Shuhua Zhang,
and Yushe Yang*Cite This: *J. Med. Chem.* 2021, 64, 8644–8665

Read Online

ACCESS |



Metrics & More

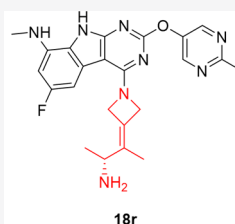


Article Recommendations

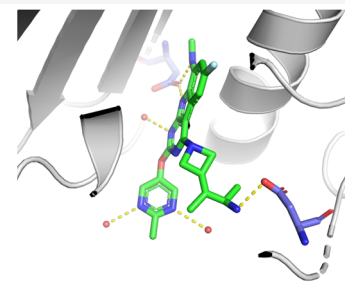


Supporting Information

ABSTRACT: Due to the poor permeability across Gram-negative bacterial membranes and the troublesome bacterial efflux mechanism, only a few GyrB/ParE inhibitors with potent activity against Gram-negative pathogens have been reported. Among them, pyrimido[4,5-*b*]indole derivatives represented by GP-1 demonstrated excellent broad-spectrum antibacterial activity against both Gram-positive and Gram-negative bacteria but were limited by hERG inhibition and poor pharmacokinetics profile. To improve their drug-like properties, we designed a series of novel pyrimido[4,5-*b*]indole derivatives based on the tricyclic scaffold of GP-1 and the C-7 moiety of acorofloxacin. These efforts have culminated in the discovery of a promising compound **18r** with reduced hERG liability and an improved PK profile. Compound **18r** exhibited superior broad-spectrum *in vitro* antibacterial activity compared to GP-1, including a variety of clinical multidrug G^- pathogens, especially *Acinetobacter baumannii*, and the *in vivo* efficacy was also demonstrated in a neutropenic mouse thigh model of infection with multidrug-resistant *A. baumannii*.



- ✓ enhanced MDR G^- bacteria activity
- ✓ reduced hERG liability
- ✓ an improved PK profile



INTRODUCTION

Antimicrobial resistance (AMR) has become one of the biggest threats to global public health over the past several decades, and we have now entered the post-antibiotic era.¹ AMR causes 700,000 or more deaths globally each year, which could increase to 10 million by 2050.² Although AMR is widespread among both Gram-positive (G^+) and Gram-negative (G^-) bacteria, the latter poses a more severe and urgent problem. This difference is derived from the outer membrane, which is a structure unique to G^- pathogens, along with efflux pumps.^{3,4} The penetration problem of G^- bacteria has been widely debated.⁵ In order to fight against AMR, it is urgent to develop novel antibiotics with new targets or new modes of action and active against resistant bacterial strains, especially G^- pathogens. Nevertheless, no new class of antibiotic against G^- pathogens has been approved in over 50 years.^{6–8} In order to guide and promote the discovery and development of novel antibiotics, the World Health Organization (WHO) has published a global priority pathogen list. Nine of the twelve important bacteria are G^- bacteria, including all three critical priority pathogens: *Acinetobacter baumannii*, *Pseudomonas aeruginosa*, and extended-spectrum β -lactamases (ESBLs) producing Enterobacteriaceae (including *Klebsiella pneumoniae* and *Escherichia coli*).⁹

DNA gyrase and topoisomerase IV are type IIA bacterial topoisomerases that have structural and functional similarities

and are vital enzymes for DNA topology and cell viability.^{10,11} GyrA/GyrB and ParC/ParE are subunits of these two enzymes, respectively. While GyrA and ParC inhibited by the well-known class of fluoroquinolones are clinically validated targets for antimicrobial agents, GyrB and ParE also have long been studied in the field of antibacterial drugs.^{12,13} Due to their different modes of action, GyrB/ParE inhibitors do not exhibit cross-resistance with fluoroquinolones.^{14,15} Varieties of novel scaffolds targeting GyrB/ParE ATP-binding site have been discovered by industry and academia during the last 50 years.¹⁴ Although several inhibitors have entered clinical trials, none of them have been approved except novobiocin (Figure 1, 1), which was withdrawn in 2011 for reasons of safety and efficacy. DS-2969b^{16,17} (2) and SPR720¹⁸ (3) are the only two compounds still in active clinical trials, while AZD-5099^{14,19} (4) entered phase I but was terminated soon after due to safety. Furthermore, few GyrB/ParE inhibitors displayed activity against critical G^- bacteria neither do the compounds

Received: April 5, 2021

Published: June 3, 2021



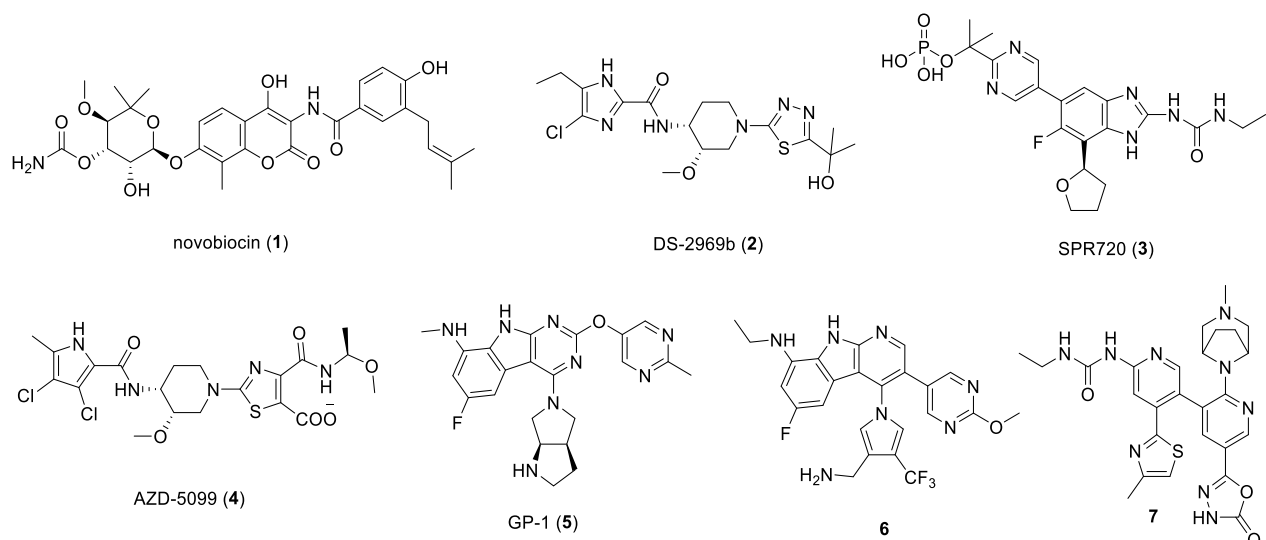


Figure 1. Structures of representative GyrB/ParE inhibitors.

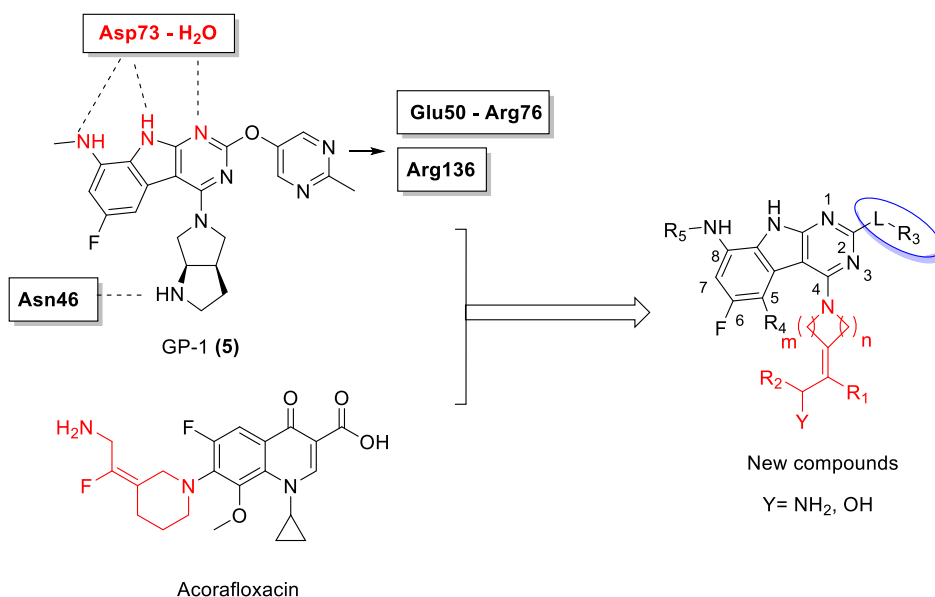
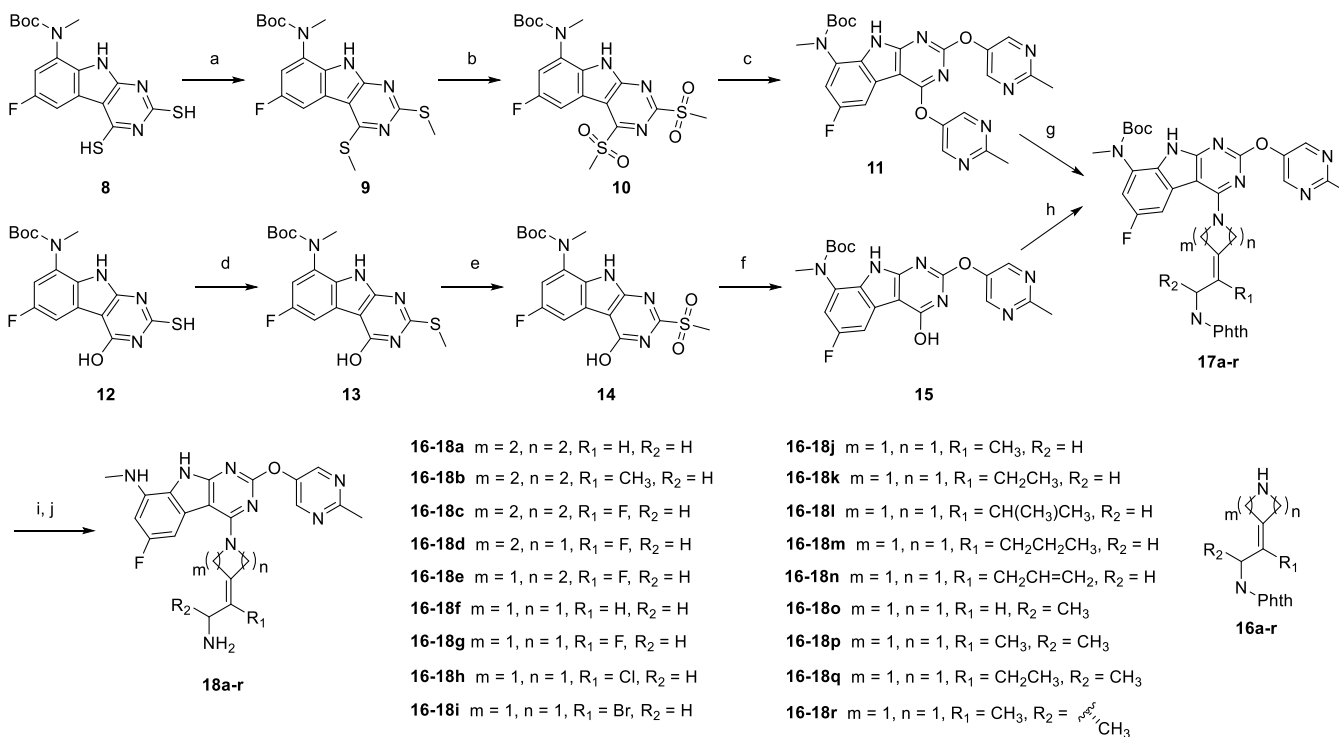


Figure 2. Design of novel pyrimido[4,5-*b*]indole GyrB/ParE inhibitors.

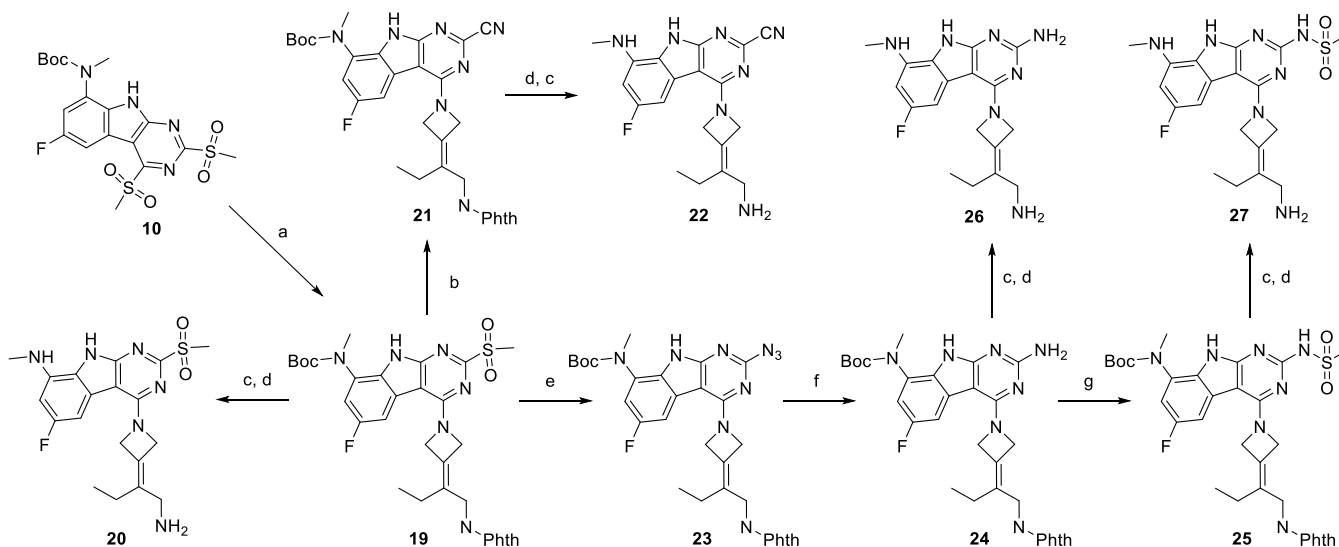
mentioned above. Pyrimido[4,5-*b*]indole inhibitors discovered by Trius Therapeutics and represented by GP-1 (5) broke this condition and showed excellent broad-spectrum activity covering *A. baumannii*, *P. aeruginosa*, and *K. pneumoniae* for the first time.²⁰ However, hERG inhibition, poor property of pharmacokinetics (PK), and insufficient efficacy *in vivo* against Gram-negative bacteria have limited the development of these compounds.^{20–22} Recently, a series of pyrido[2,3-*b*]indole derivatives²³ represented by compound 6 and pyridylurea derivatives²⁴ represented by compound 7 were also demonstrated to have strong activity against critical G⁻ pathogens *in vitro*. According to the “rules of penetration”,²⁵ the unique G⁻ activities of these compounds probably originate from the high rigidity and low three-dimensionality of their structures with an ionizable nitrogen. Nevertheless, the *in vivo* potency remains a problem.

The X-ray crystal structure of GP-1 in complex with *E. coli* GyrB²⁰ shows that the pyrimido[4,5-*b*]indole scaffold binds to the ATP-binding site of GyrB, forming hydrogen bonds with

the Asp73 carboxylate group and a conserved water molecule, which are crucial to its antibacterial activity, while the methyl pyrimidine moiety at the C-2 position is involved in interactions with Glu50-Arg76 and Arg136 (Figure 2). The basic amino moiety at the C-4 position is shown to interact with Asn46 within a structured water network, which is considered to be important for activity against G⁻ bacteria.²⁰ In an attempt to overcome the drawbacks of pyrimido[4,5-*b*]indole derivatives, GP-1 was selected as the lead compound and modifications at the C-2, C-4, C-5, and C-8 were designed (Figure 2). Actually, the (3*aR*,6*aR*)-octahydropyrrolo[3,4-*b*]pyrrole moiety of GP-1 was derived from the basic amino moiety at the C-7 position of fluoroquinolone. According to the interactions demonstrated above and the C-7 position modification of acorafloxacin,²⁶ a unique C-4 moiety was introduced in the new design (Figure 2). Acorafloxacin had entered phase II clinical trials and its C-7 moiety is featured with the exocyclic double bond, with which the chemical

Scheme 1. Synthesis of Compounds 18a–r^a

^aReagents and conditions: (a) MeI, K₂CO₃, DMF, 0 °C, 94%; (b) mCPBA, DCM, 0 °C to rt, 84%; (c) 2-methylpyrimidine-5-ol, K₂CO₃, NMP, 100 °C, 84%; (d) MeI, K₂CO₃, DMF, 0 °C, 78%; (e) mCPBA, DMF, 0 °C to rt, 85%; (f) 2-methylpyrimidine-5-ol, K₂CO₃, NMP, 100 °C, 81%; (g) **16a–b**, **16f**, **16j–k**, and **16m–r**, K₂CO₃, NMP, microwave at 100 °C; (h) BOP, **16c–e**, **16g–i**, and **16l**, triethylamine, NMP, 0 to 50 °C; (i) TFA, DCM, rt; (j) hydrazine hydrate for **18a–m** and **18o–r**, MeOH, reflux, 9–82% for three steps; methylamine for **18n**, EtOH, 40 °C, 30% for three steps.

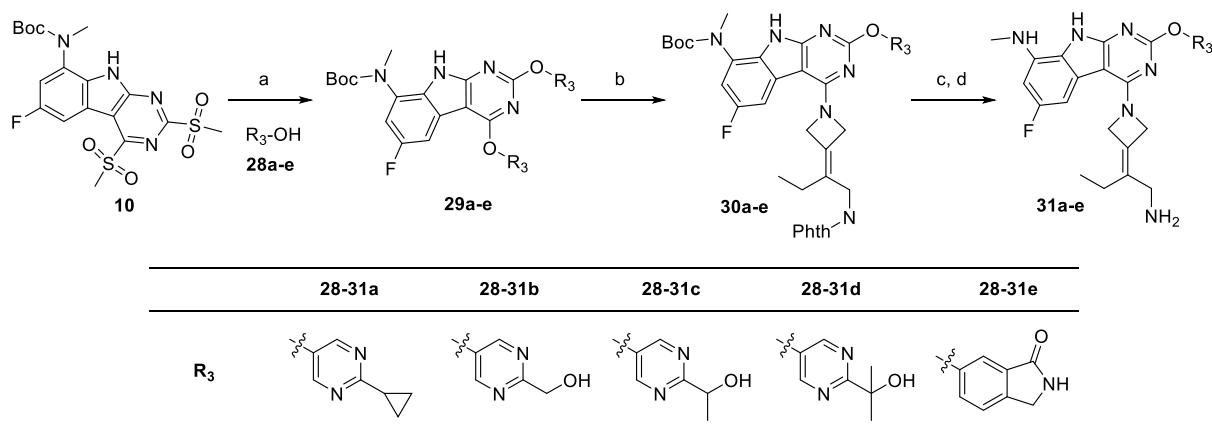
Scheme 2. Synthesis of Compounds 20, 22, and 26–27^a

^aReagents and conditions: (a) **16k**, K₂CO₃, NMP, 100 °C, 67%; (b) NaCN, DMSO, 95 °C, 86%; (c) TFA, DCM, rt; (d) hydrazine hydrate, MeOH, reflux, 12–62% for three steps.; (e) NaN₃, DMSO, 60 °C, 94%; (f) H₂, Pd/C, EtOH, rt, 66%; (g) methanesulfonyl chloride, triethylamine, pyridine, sealed tube, 90 °C, 32%.

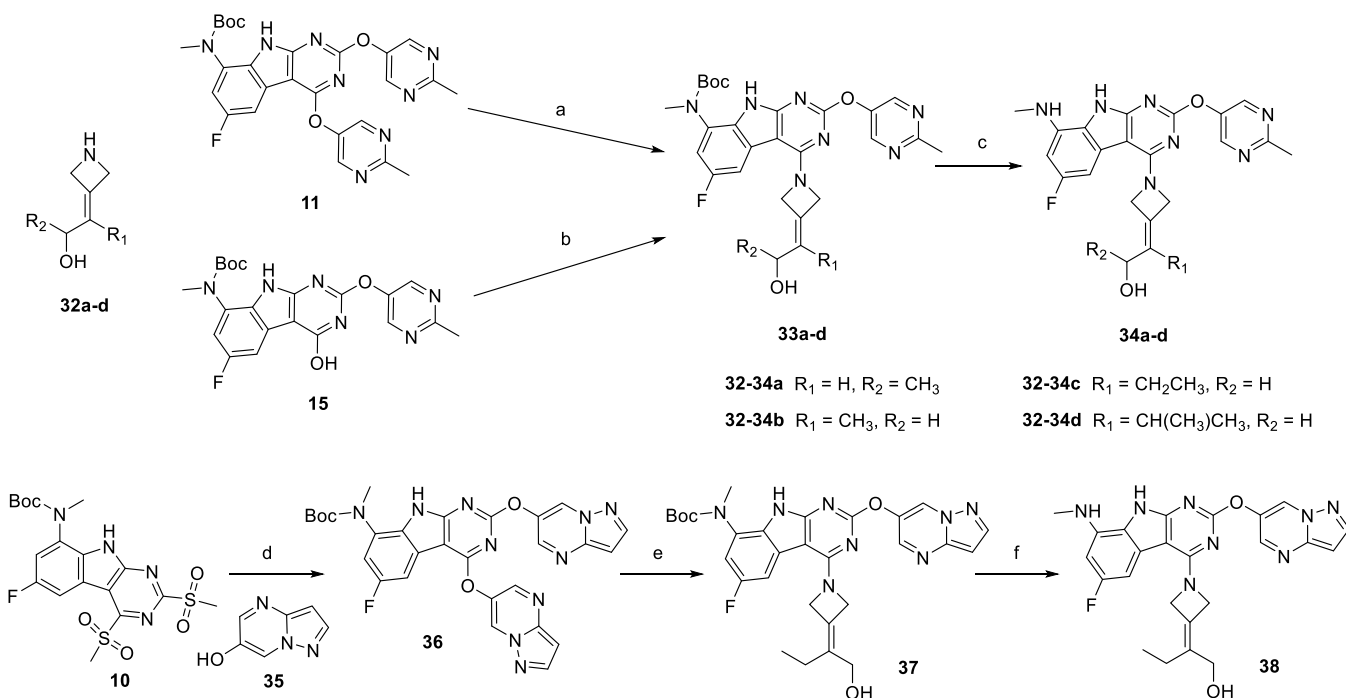
structural novelty of new compounds could be improved and the antibacterial activity could be changed.

As previous observations^{27,28} have revealed that the inhibitory activity against DNA gyrase had minor correlation with the antibacterial activity, phenotypic screening (MIC test) was employed in our research, which is the most widely

accepted method to discover novel antibacterial agents. Herein, we demonstrated our effort in discovering a series of novel pyrimido[4,5-*b*]indole derivatives with superior G⁻ bacterial activity, low hERG inhibition, and improved PK properties in rodent models. Among them, efficacy of compound **18r** was also studied *in vivo*.

Scheme 3. Synthesis of Compounds 31a–e^a

^aReagents and conditions: (a) **28a–e**, K₂CO₃, NMP, 100 °C; (b) **16k**, K₂CO₃, NMP, microwave at 100 °C; (c) TFA, DCM, rt; (d) hydrazine hydrate, MeOH, reflux, 15–34% for four steps.

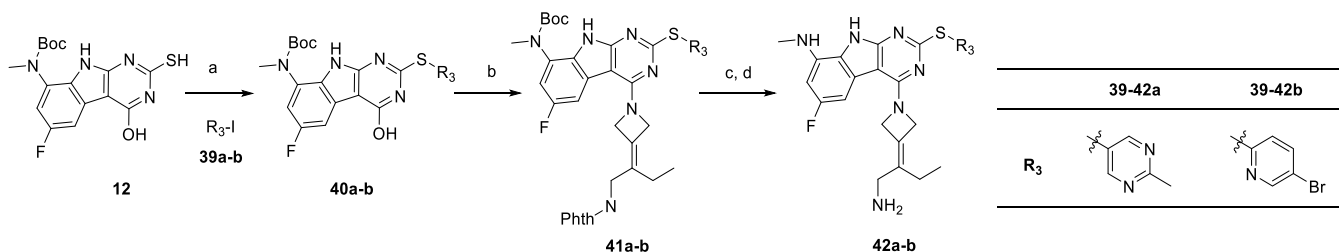
Scheme 4. Synthesis of Compounds 34a–d and 38^a

^aReagents and conditions: (a) **32a–c**, K₂CO₃, NMP, microwave at 100 °C; (b) BOP, **32d**, triethylamine, NMP, 0 to 50 °C; (c) TFA, DCM, rt, 20–31% for two steps; (d) **35**, K₂CO₃, NMP, microwave at 100 °C, 82%; (e) **32c**, K₂CO₃, NMP, microwave at 100 °C; (f) TFA, DCM, rt, 32% for two steps.

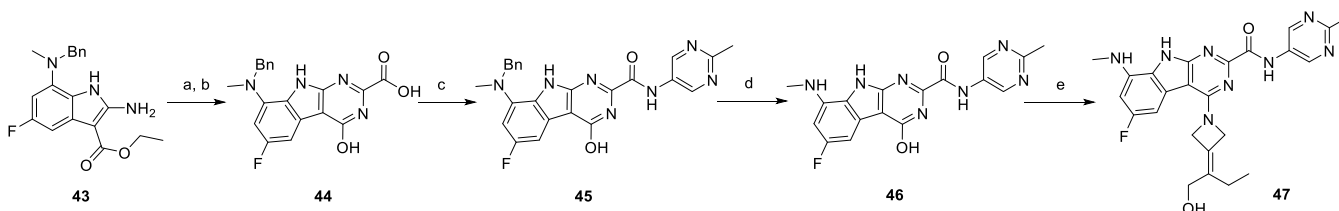
CHEMISTRY

The preparation of compounds **18a–r** is illustrated in Scheme 1. Methyl sulfide **9** was afforded from methylation of **8**²⁹ with iodomethane. In the presence of 3-chloroperoxybenzoic acid (mCPBA), **9** was oxidized to methylsulfonyl intermediate **10**. Via a substitution reaction with 2-methylpyrimidine-5-ol at the C-2 position and C-4 position of **10**, key intermediate **11** was obtained. In the other branch, thiol compound **12**²⁹ was converted to methyl sulfide **13** when one equivalent of iodomethane was added. **13** was oxidized to **14** with mCPBA in an ice-water bath. Key intermediate **15** was then prepared through a substitution reaction with 2-methylpyrimidine-5-ol at the C-2 position of **14**, similar to the synthesis of **11**. Based

on these key intermediates (**10**, **11**, and **15**), a series of pyrimidoindole compounds modified at the C-2 and C-4 positions were synthesized. With the installation of aliphatic amines **16a–r** by condensation or selective substitution reactions at the C-4 position, compounds **17a–r** were prepared from **11** or **15**. The condensation reactions were activated by the benzotriazol-1-yloxytris(dimethylamino)-phosphonium hexafluorophosphate (BOP) reagent and the substitution reactions took place under microwave irradiation at 100 °C. Compounds **18a–r** were prepared after *tert*-butoxycarbonyl (Boc) and phthaloyl (Phth) were subsequently deprotected. Compounds **18a–b**, **18f**, **18j–k**, and **18m–r** were obtained via key intermediate **11**, but compounds **18c–e**, **18g–i**, and **18l** failed to be prepared by the same route and

Scheme 5. Synthesis of Compounds 42a–b^a

^aReagents and conditions: (a) 39a–d, K₂CO₃, CuI, PPh₃, (1*R*,2*R*)-*N,N'*-dimethyl-1,2-cyclohexanediamine, NMP, 130 °C; (b) BOP, 16k, triethylamine, NMP, 0 to 50 °C, 20–40% for two steps; (c) TFA, DCM, rt; (d) hydrazine hydrate, MeOH, reflux, 57–61% for two steps.

Scheme 6. Synthesis of Compound 47^a

^aReagents and conditions: (a) NCCOOEt, 4 N HCl in 1,4-dioxane, 82 °C; (b) 10% NaOH (aq), EtOH, reflux, 97% for two steps; (c) 2-methyl-5-pyrimidinamine, HATU, triethylamine, DMF, rt, 14%; (d) H₂, 10% Pd/C, 50 °C, 58%; (e) BOP, 32c, triethylamine, NMP, 0 to 50 °C, 20%.

were instead prepared from intermediate 15. An ee value greater than 94% was achieved during the preparation of compound 18r. Details for the synthesis of aliphatic amines 16a–r can be found in the [Supporting Information](#).

The divergent synthesis of analogues with various functional groups at the C-2 position is illustrated in [Scheme 2](#). Intermediate 10 was selectively reacted with 16k at the C-4 position to afford key intermediate 19, which was then deprotected by TFA and hydrazine hydrate to produce compound 20. Intermediate 19 was exposed to sodium cyanide in DMSO at 95 °C to obtain intermediate 21, followed by deprotection of the Phth and Boc groups to give compound 22. Intermediate 19 was also substituted with NaN₃ in DMSO at 60 °C and reduced by H₂ with palladium on carbon to obtain amine derivative 24, which was subsequently reacted with methanesulfonyl chloride in a sealed tube to provide sulfamide 25. Compounds 26 and 27 were produced after deprotection of amine 24 and sulfamide 25, respectively.

Analogues 31a–e were prepared from intermediate 10 ([Scheme 3](#)). This key intermediate reacted with 28a–e to afford 29a–e and then underwent substitution with amine 16k at the C-4 position to obtain 30a–e. Subsequent removal of the Boc- and Phth-protecting groups with TFA and hydrazine hydrate provided compounds 31a–e. Compounds 28a and 28e were purchased, while intermediates 28b–d were synthesized, the details of which can be found in the [Supporting Information](#).

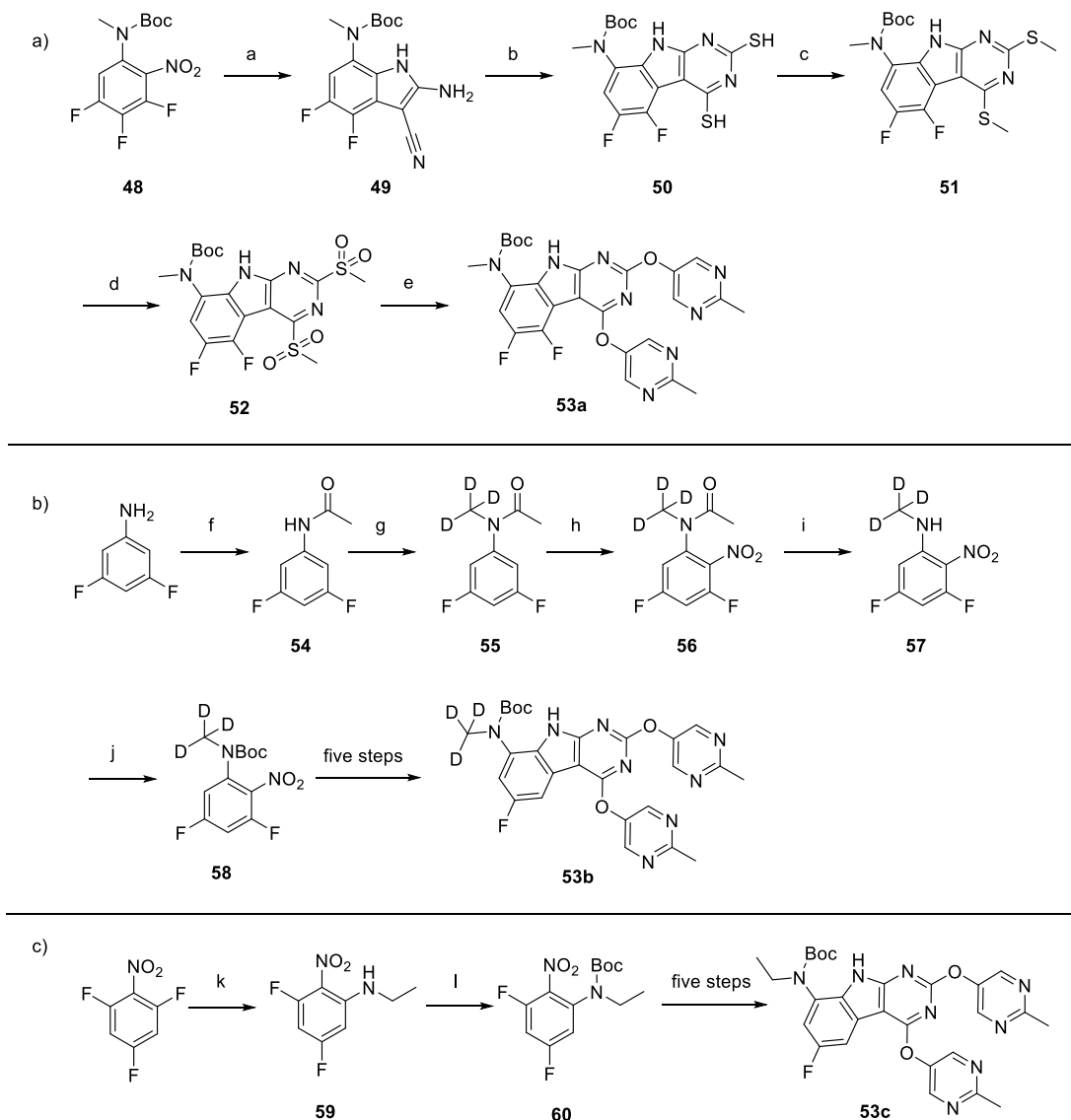
The procedures for the synthesis of compounds 34a–d and 38 are depicted in [Scheme 4](#) and are similar to those for 18a–r. Compounds 33a–d were also prepared from the key intermediates 11 or 15 by condensation or substitution with aliphatic alcohols 32a–d. Analogues 34a–d were obtained after final deprotection with TFA for 2 min. As the C-4 moiety containing a hydroxy group would be cleaved by TFA, the reaction time should be controlled. Key intermediate 10 was reacted with 35 to afford intermediate 36. After substitution to a

substitution reaction with 32c followed by deprotection, 36 was converted to compound 38.

The synthesis routine toward C-2 thioether analogues 42a–b is illustrated in [Scheme 5](#). The thiol group in 12 underwent an Ullmann coupling reaction with the corresponding iodide 39a–b to provide thioether intermediates 40a–b. CuI, PPh₃, and (1*R*,2*R*)-*N,N'*-dimethyl-1,2-cyclohexanediamine were engaged in the coupling. Via a condensation reaction with the BOP reagent, amine 16k was installed at the C-4 position of 40a–b to afford 41a–b. Subsequent Boc and Phth deprotection led to the formation of compounds 42a–b.

Compound 47 with an amide linker was prepared from indole 43 as outlined in [Scheme 6](#). Intermediate 43²⁹ was reacted in a solution of 4 M hydrogen chloride in 1,4-dioxane with ethyl cyanofornate to produce acid 44. In the presence of 2-(7-azabenzotriazol-1-yl)-*N,N,N',N'*-tetramethyluronium hexafluorophosphate (HATU) and triethylamine, a condensation reaction between acid 44 and 2-methyl-5-pyrimidinamine afforded amide 45. Catalyzed by 10% palladium on carbon, the benzyl group of intermediate 45 was deprotected to obtain amide 46 under a hydrogen atmosphere. After condensing 32c with BOP, amide 46 was converted to compound 47.

The synthesis of three key intermediates 53a–c is displayed in [Scheme 7](#). Trifluoride 48²⁹ was substituted by malononitrile at the C-3 position by an S_NAr reaction in the presence of NaOH and then reduced by sodium dithionite to afford cyanide 49. Catalyzed by DMSO, intermediate 49 reacted with carbon disulfide (CS₂) in a sealed tube to form a pyrimidoindole and provide dithiol 50. Difluoride 52 was obtained via subsequent methylation by MeI and oxidation by mCPBA. 2-Methylpyrimidine-5-ol was installed at the C-2 and C-4 positions of the pyrimidoindole to afford 53a. The first five steps of the synthesis of deuterated intermediate 53b were different, with 3,5-difluoroaniline as the starting material. Acetic anhydride was used to acetylate 3,5-difluoroaniline and then deuterated iodomethane was used to obtain difluoride 55. In concentrated sulfuric acid, difluoride 56 was produced after

Scheme 7. Synthesis of Key Intermediates 53a–c^a

^aReagents and conditions: (a) malononitrile, NaOH, NaHCO₃, sodium dithionite, DMF, 0 to 40 °C, 71%; (b) CS₂, NaOH, DMSO, EtOH, 80 °C; (c) MeI, K₂CO₃, DMF, 0 °C, 42% for two steps; (d) mCPBA, DCM, 0 °C to rt, 51%; (e) 2-methylpyrimidine-5-ol, K₂CO₃, NMP, 100 °C, 55%; (f) acetic anhydride, 0 °C, 83%; (g) deuterated iodomethane, NaH, THF, 0 °C, 60%; (h) KNO₃, conc. H₂SO₄, 0 °C, 62%; (i) 4 M HCl (aq), 1,4-dioxane, reflux, 94%; (j) Boc₂O, NaH, THF, 0 °C to rt, 82%; (k) ethylamine, THF, 0 °C, 70%; (l) Boc₂O, DMAP, THF, 0 °C to rt, 58%.

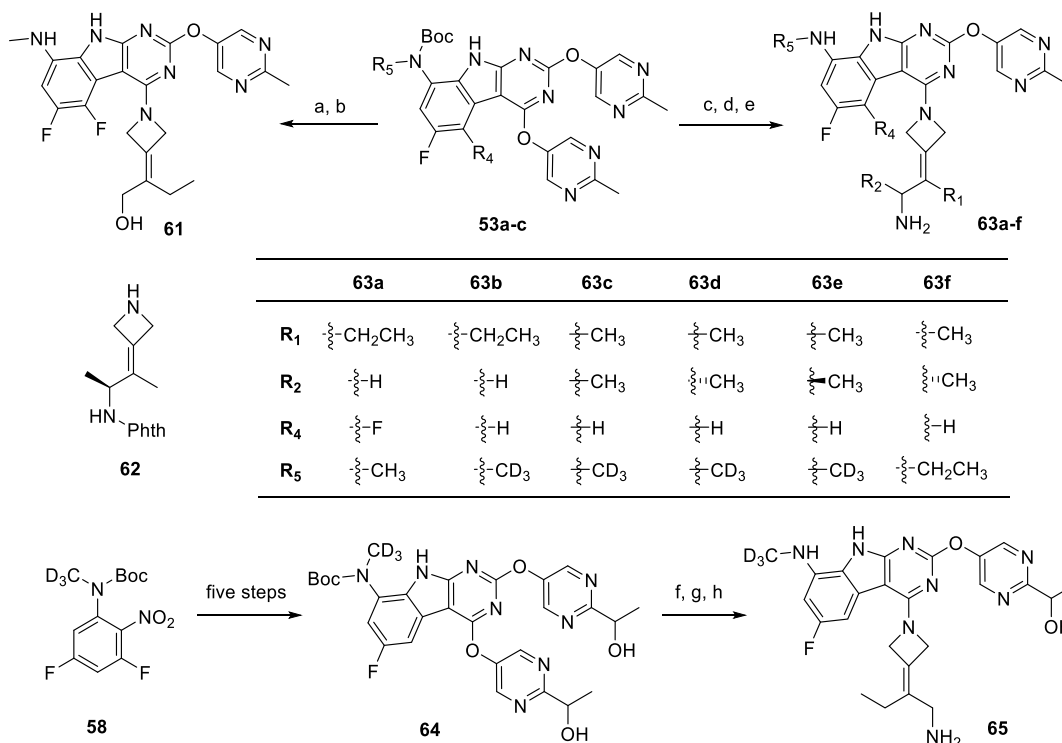
nitration of **55** in the presence of potassium nitrate. Acetyl-**56** was deprotected by 4 M HCl (aq), and the naked amino was subsequently Boc-protected to afford difluoride **58**. In this reaction, 4-dimethylaminopyridine (DMAP) did not work well, and NaH was chosen to facilitate the effects of Boc₂O. Key intermediate **56b** was then accessed through a five-step synthetic sequence similar to that for **56a**. Difluoride **59** was prepared from 1,3,5-trifluoro-2-nitrobenzene by an S_NAr reaction with ethylamine. Difluoride **60** was afforded via Boc protection catalyzed by DMAP. Key intermediate **56c** was then obtained through a five-step process similar to that for **56a** outlined in Scheme 7a.

The synthesis of analogues **61**, **63a–f**, and **65** is shown in Scheme 8. Intermediate **53a** was substituted by **32c** and then deprotected to afford compound **61**. With the participation of amines **16k**, **16p**, **16r**, and **62**, compounds **63a–f** were accessed by carrying **53a–c** through the three-step synthetic

sequence (g–i) outlined in Scheme 1. The ee values of compounds **63d–e** were both greater than 92%. Intermediate **64** was prepared from difluoride **58** through a five-step synthetic process similar to that of **56a**, as shown in Scheme 7a. Compound **65** was then produced after installation of **16k** at the C-4 position of **64** along with Boc and Phth deprotection.

RESULTS AND DISCUSSION

SARs and hERG Inhibition of the Newly Synthesized Pyrimidoindoles. The *in vitro* activities of all new pyrimidoindoles were evaluated. To better correlate the *in vitro* activities with future clinical applications, most of the tested bacterial strains were clinical isolates, including fluoroquinolone-resistant and methicillin-resistant *Staphylococcus aureus* (MRSA), ESBL-producing *E. coli*, oxacillinase (OXA-23)-producing multidrug-resistant (MDR) *A. baumann-*

Scheme 8. Synthesis of Compounds 61, 63a–f, and 65^a

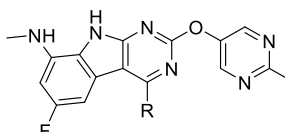
^aReagents and conditions: (a) **32c**, K₂CO₃, NMP, microwave at 100 °C; (b) TFA, DCM, rt, 21% for two steps; (c) **16k**, **16p**, **16r** and **62**, K₂CO₃, NMP, microwave at 100 °C; (d) TFA, DCM, rt; (e) hydrazine hydrate, MeOH, reflux, 10–38% for three steps; (f) **16k**, K₂CO₃, NMP, microwave at 100 °C; (g) TFA, DCM, rt; (h) hydrazine hydrate, MeOH, reflux, 24% for three steps.

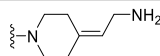
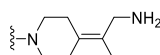
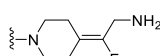
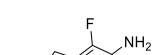
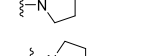
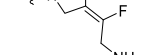
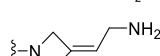
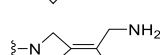
nii, imipenemase (IMP-4)-producing MDR *P. aeruginosa*, and *K. pneumoniae* carbapenemase (KPC-2)-producing MDR *K. pneumoniae*. We also tested compounds with standard strains, such as *E. coli* ATCC35218. The activities are presented as the minimum inhibitory concentrations (MICs), and the results are displayed as ranges of MIC values. The racemate of GP-1 was used here as a positive control. More details about the antibacterial activity and strains can be found in the [Supporting Information](#).

The C-4 moiety on pyrimidoindole is essential for antibacterial activity, especially the G⁻ bacterial activity, and can modulate metabolic property, safety, antibacterial spectrum, and structure novelty by diversified substituents. Trius Therapeutics have explored varieties of saturated cyclo-heteroaliphatic amine rings in this position, including single rings, fused rings, bridge rings, and spiro rings, but failed to balance the activity against G⁻ pathogens and hERG inhibition.²⁹ We wanted to not only improve the activity but also evade the hERG K⁺ channel inhibition problem that exists in pyrimido[4,5-*b*]indole series. Inspired by the patent of acorofloxacin,³⁰ we modified the C-4 moiety with an exocyclic double bond linked to the ring system for the initial investigation, as shown in [Table 1](#). By adjusting the ring size with the change in *m* and *n*, we first explored the effect of azetidine, pyrrolidine, and piperidine rings. The different broad-spectrum performances of compounds **18a–g** demonstrated that the pyrrolidine ring was most beneficial for activity, and azetidine was the second. However, the hERG inhibition results of **18c**, **18e**, and **18g** in [Table 2](#) showed that the azetidine had less hERG liability than the pyrrolidine or piperidine scaffold, especially the compound **18g** whose maximum inhibition rate was as low as 3.2%. The hERG

inhibition problem was surprisingly solved by the azetidine ring at the beginning of our exploration. Combined with its advantages in configuration and metabolic stability, the azetidine ring provided more attractive potential for further investigation. Additionally, CH₃ and F substituents at the R1 position contributed significant improvement in antibacterial activity and indicated that the R1 position deserved more modifications.

Based on the azetidine ring, a comprehensive SAR investigation was implemented around the C-4 moiety on R1 and R2, as displayed in [Table 3](#). Since the G⁺ bacterial activity demonstrated by **18g** was potent enough, we cast more attention to improve the activity against G⁻ pathogens. To our delight, analogues **18i** and **18k–o** exhibited superior broad-spectrum antibacterial activity over *rac*-GP-1, especially against ECO⁺. Compared to **18g**, Cl and Br substitutions, as in **18h** and **18i**, improved the *S. aureus* and ECO⁺ activity, suggesting that weak electron-withdrawing groups are preferred. However, the corresponding C-4 moieties **16h–i** were not used in later investigations because the physicochemical properties of **18h–i** were poor. Compound **18j**, with a methyl substitution on the double bond, showed better antibacterial activity than **18f** but was not as potent as *rac*-GP-1 in G⁻ activity. Surprisingly, the ethyl group of **18k** led to a large improvement in activity against G⁻ bacteria, which was 2–64-fold more potent than *rac*-GP-1. After that, the effects of isopropyl, *n*-propyl, and allyl groups at R1 were studied. Compounds **18l–n** all demonstrated excellent G⁻ activity, although they were less potent than **18k**, indicating that hydrophobic R1 groups were tolerated. Due to the relatively high hERG inhibition of compounds **18m–n**, substitutions larger than *n*-propyl were not tried.

Table 1. *In Vitro* Antibacterial Activity of Compounds 18a–g


| Compd | R | MIC (μg/mL) ^a | | | | | | |
|--------------|---|--------------------------|------------|--------------|--------------|------------------|------------------|-------|
| | | MRSA | MSSA | MRSE | MSSE | ECO ⁺ | ECO ⁻ | PAE |
| 18a |  | 0.5-2 | 1-2 | 0.25-0.5 | 0.25 | 8-16 | 2->16 | ≥16 |
| 18b |  | 0.125-0.5 | 0.125-0.25 | <0.008 | 0.03 | 2-4 | 0.25-2 | 8->16 |
| 18c |  | 0.015-0.125 | 0.015 | <0.008 | <0.008 | 0.5-1 | 0.06-1 | 8->16 |
| 18d |  | <0.008 | <0.008 | <0.008 | <0.008 | 0.125-0.25 | <0.008-0.5 | 2-8 |
| 18e |  | <0.008 | <0.008 | <0.008 | <0.008 | 0.015-0.06 | <0.008-0.06 | 2-4 |
| 18f |  | 0.5-2 | 0.5-1 | 0.25 | 0.25 | 8-16 | 0.5-16 | ≥16 |
| 18g |  | 0.015-0.125 | 0.06-0.25 | 0.015-1 | 0.125 | 0.25-0.5 | 0.06-0.5 | >16 |
| rac-GP-1 |  | 0.015-0.06 | <0.008 | <0.008-0.015 | <0.008-0.015 | 0.25-1 | 0.06-0.5 | 0.5-2 |
| Levofloxacin | | 16-64 | 0.25-8 | 4->64 | 0.125-4 | 0.5-16 | ≤0.03->64 | 0.5-4 |

^aMRSA, methicillin-resistant *S. aureus*, 4 strains; MSSA, methicillin-sensitive *S. aureus*, 4 strains; MRSE, methicillin-resistant *S. epidermidis*, 4 strains; MSSE, methicillin-sensitive *S. epidermidis*, 4 strains; ECO⁺, ESBL-producing *E. coli*, 3 strains; ECO⁻, non-ESBL-producing *E. coli*, 3 strains; and PAE, IMP-4 producing MDR *P. aeruginosa*, 3 strains.

Table 2. hERG K⁺ Channel Inhibition of Selected Compounds^a

| compd | maximum inhibition rate (%) | IC ₅₀ (μM) |
|-----------|-----------------------------|-----------------------|
| 18c | 70.4 | 18.4 |
| 18e | 41.6 | >40 |
| 18g | 3.2 | >40 |
| 18h | 34.3 | >40 |
| 18j | 4.8 | >40 |
| 18k | 41.1 | >40 |
| 18l | 26.5 | >40 |
| 18m | 50.6 | 51.5 |
| 18n | 49.1 | >40 |
| 18o | 32.3 | >40 |
| 18p | 37.0 | >40 |
| 18r | 18.3 | >40 |
| 31a | 62.0 | 23.4 |
| 31b | 30.9 | >40 |
| 31c | 36.0 | >40 |
| 63c | 14.2 | >40 |
| rac-GP-1 | 70.5 | 12.3 |
| Cisapride | 97.7 | 0.04 |

^aThe maximum tested concentration of cisapride was 3 μM, and the maximum tested concentrations of the other compounds were 40 μM.

With regard to another position, R2 of the C-4 moiety, subtle modifications could greatly influence the potency *in vitro*. Compared to 18j, a methyl group at the R2 position of

compound 18o significantly improved G⁻ activity with a 4–16-fold potency shift in the MIC. Compound 18p, which is a racemate, was designed and synthesized based on compound 18o and maintained potency under the effect of a methyl group at R1. Nevertheless, the introduction of an ethyl group at R2 (18q) led to a great decrease in activity, especially for G⁻ pathogens, indicating that a large group was not tolerated at the R2 position. Compounds 18h and 18j–p were also tested for their inhibition of the hERG K⁺ channel, and their IC₅₀ values were all greater than the highest tested concentration (40 μM), suggesting good safety to a certain degree.

Given the solubilities of pyrimido[4,5-*b*]indole derivatives were generally very poor and compounds with hydroxy groups could be readily transformed into prodrugs whose water solubility would be significantly improved, compounds 34a–d with terminal hydroxy groups at the Y position in the C-4 moiety were prepared. These compounds suffered a significant loss in activity against G⁻ bacteria compared with their amine analogues, especially for *P. aeruginosa*, further proving that terminal amines in the C-4 moiety are of importance to G⁻ bacterial activity. However, hydroxyl groups would show an advantage when another fluorine atom was installed at the C-5 position of the pyrimidoindole, since the activity of hydroxy compound 61 was much better than that of amine 63a. Compared to compound 18k, amine 63a lost most activity, indicating that the hydrogen atom at the C-5 position was more beneficial than the fluorine atom in this series.

Table 3. *In Vitro* Antibacterial Activity of Compounds 18h–q, 34a–d, 61, and 63a^a

| compd | R1 | R2 | R4 | MIC ($\mu\text{g/mL}$) ^a | | | | | | |
|--------------|-------|-------|------------|---------------------------------------|--------------|--------------|------------------|------------------|------------------|-----------|
| | | | | MSSA | MRSA | MSSE | MRSE | ECO ⁺ | ECO ⁻ | PAE |
| 18h | Cl | H | H | <0.008 | <0.008 | <0.008 | <0.008 | 1 | 0.25–2 | 8–16 |
| 18i | Br | H | H | <0.008 | <0.008 | <0.008 | <0.008 | 0.06–0.5 | 0.015–0.5 | 2–4 |
| 18j | Me | H | H | <0.008–0.015 | 0.015–0.06 | <0.008 | <0.008 | 2–4 | 0.06–1 | 4–>16 |
| 18k | Et | H | H | <0.008 | <0.008 | <0.008 | <0.008 | <0.008–0.015 | <0.008–0.06 | 0.5–1 |
| 18l | i-Pr | H | H | <0.008 | <0.008 | <0.008 | <0.008 | 0.125–0.25 | 0.03–0.5 | 1–2 |
| 18m | n-Pr | H | H | <0.008 | <0.008 | <0.008 | <0.008 | 0.125–0.25 | 0.06–0.5 | 2 |
| 18n | allyl | H | H | <0.008 | <0.008 | <0.008 | <0.008 | 0.125–0.25 | 0.06–0.5 | 1 |
| 18o | H | Me | H | <0.008 | <0.008 | <0.008 | <0.008 | 0.125–0.25 | 0.015–0.25 | 0.5–1 |
| 18p | Me | Me | H | <0.008–0.015 | <0.008 | <0.008 | <0.008 | 0.5–1 | 0.25–1 | 1–2 |
| 18q | Et | Me | H | 0.5 | 0.25–0.5 | 0.03–0.125 | 0.03–0.25 | ≥ 16 | 8–>16 | >16 |
| 34a | H | Me | H | <0.008 | <0.008 | <0.008 | <0.008 | 0.5–1 | 0.125–1 | >16 |
| 34b | Me | H | H | <0.03 | <0.03 | <0.03 | <0.03 | >64 | 0.25–>64 | >64 |
| 34c | Et | H | H | <0.008 | <0.008 | <0.008 | <0.008 | 0.25–0.5 | 0.125–0.5 | 4–16 |
| 34d | i-Pr | H | H | <0.03 | <0.03 | <0.03 | <0.03 | 0.5–1 | 0.25–1 | ≥ 64 |
| 61 | Et | H | F | <0.03 | <0.03 | <0.03 | <0.03 | 0.25–0.5 | 0.125–1 | 8–>64 |
| 63a | Et | H | F | 0.25–2 | 0.25–0.5 | <0.03 | <0.03–2 | 64 | 32–64 | >64 |
| rac-GP-1 | | | 0.015–0.06 | <0.008 | <0.008–0.015 | <0.008–0.015 | 0.25–1 | 0.06–0.5 | 0.5–2 | |
| levofloxacin | | 16–64 | 0.25–8 | 4–>64 | 0.125–4 | 0.5–16 | ≤ 0.03 –>64 | 0.5–4 | | |

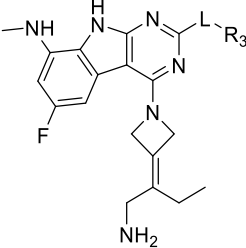
^aMRSA, methicillin-resistant *S. aureus*, 4 strains; MSSA, methicillin-sensitive *S. aureus*, 4 strains; MRSE, methicillin-resistant *S. epidermidis*, 4 strains; MSSE, methicillin-sensitive *S. epidermidis*, 4 strains; ECO⁺, ESBL-producing *E. coli*, 3 strains; ECO⁻, non-ESBL-producing *E. coli*, 3 strains; and PAE, IMP-4 producing MDR *P. aeruginosa*, 3 strains.

According to explorations of Trius Therapeutics²⁹ and Redx Pharma,³¹ modification in the C-2 moiety could greatly influence the antibacterial activity. Given the encouraging outcome of 18k, its C-4 moiety was fixed in our following investigation of the C-2 moiety. Table 4 shows the *in vitro* activity of compounds with modifications to L and R₃. Methylsulfonyl, cyano, amino, and methanesulfonamide groups were explored at the C-2 position, but these compounds (20, 22, and 26–27) lost almost all activity, indicating that aromatic rings in the C-2 moiety were required for potency. With a cyclopropyl group introduced at the pyrimidine of the C-2 moiety, compound 31a still exhibited better potency than rac-GP-1 but had moderate inhibition of the hERG K⁺ channel with an IC₅₀ of 23.4 μM . Hence, we fine-tuned the substitution at the 2'-position on the pyrimidine of R3 where the vector is pointing toward the solvent-exposed area. Hydroxymethyl groups and 1-hydroxyethyl groups at this position (31b and 31c) could maintain potency against G⁺ bacteria but partly lost potency against ECO⁻ and *P. aeruginosa* compared to rac-GP-1. The antibacterial activity of 31d with a 2-hydroxypropan-2-yl group suffered a larger decrease in activity against G⁻ pathogens, which was in accordance with the research by Hu et al.²³ Compounds 31b–c performed well in the hERG inhibition assay and further suggested that the azetidine moiety resolved the hERG inhibition problem. Compound 31e with an aliphatic ring fused to a benzene ring and compound 42b with 5-bromopyridin-2-yl lost most activity, while compound 38, with pyrazolo[1,5-a]pyrimidinyl,

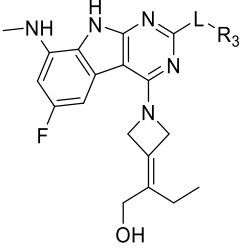
retained activity compared to 34c with a methyl pyrimidine moiety. Ether, thioether, and amide linkers (such as compounds 18k, 42a, and 47) were investigated at the L position, and the ether moiety proved to be the best linker among them. While a thioether led to a slight reduction in potency, the amide linker resulted in a total loss of activity against G⁻ bacteria. The SARs at C-2 of the pyrimidopyrimidinones indicated that the (2-methylpyrimidin-5-yl)oxy moiety of 18k seemed to be the optimal selection.

According to the excellent data shown above, compounds 18k–p and 31b–c were selected to test against more strains and species of G⁻ bacteria (Table 5, more results are detailed in the Supporting Information; the MDR *E. coli* and *P. aeruginosa* tested in this table are different from the strains tested in Tables 1, 3, and 4). These compounds all exhibited broad-spectrum antibacterial activity covering all three critical priority pathogens emphasized by the WHO, especially MDR *A. baumannii*. In this test, the potency of compound 18k was 2–8-fold stronger than that of rac-GP-1, while the activities of 18n, 18p, and 31c were comparable to this lead compound. We also compared these compounds with meropenem and cefiderocol which is a novel antibiotic potent against critical MDR G⁻ pathogens, and our compounds showed significant superior activity *in vitro* over these controls. The great difference in activity between levofloxacin and these compounds further proved their quite different mechanisms of action.

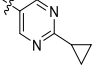
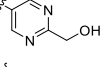
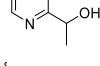
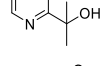
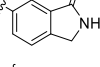
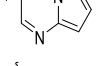
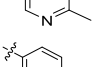
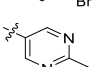
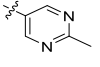
Table 4. *In Vitro* Antibacterial Activity of Compounds 20, 22, 26–27, 31a–e, 38, 42a–b, and 47^a



20, 22, 26-27, 31a-e, 42a-b



38, 47

| Compd | L | R ₃ | MIC (μg/mL) ^a | | | | | | |
|--------------|---|---|--------------------------|--------------|--------------|--------------|------------------|------------------|-------|
| | | | MSSA | MRSA | MSSE | MRSE | ECO ⁺ | ECO ⁻ | PAE |
| 20 | / | SO ₂ CH ₃ | >16 | >16 | >16 | >16 | >16 | >16 | >16 |
| 22 | / | CN | 2 | 1-2 | 0.25-1 | 0.5-2 | 0.5-8 | 0.25-8 | 16 |
| 26 | / | NH ₂ | 4->16 | 4 | 2-16 | 4 | 4-16 | 2-16 | ≥16 |
| 27 | / | NHSO ₂ CH ₃ | >16 | >16 | >16 | >16 | >16 | >16 | >16 |
| 31a | O |  | <0.008 | <0.008 | <0.008 | <0.008 | 0.03-0.125 | 0.015-0.125 | 0.5-1 |
| 31b | O |  | <0.008 | <0.008 | <0.008 | <0.008 | 0.5-1 | 0.25-2 | 4->16 |
| 31c | O |  | <0.008 | <0.008 | <0.008 | <0.008 | 0.5-1 | 0.25-2 | 16 |
| 31d | O |  | <0.008 | <0.008 | <0.008 | <0.008 | 1 | 0.5-1 | >16 |
| 31e | O |  | 0.5-1 | 0.5-2 | 0.06-0.5 | 0.06-0.5 | 8-16 | 8->16 | 16 |
| 38 | O |  | <0.015 | <0.015 | <0.015 | <0.015 | 0.25-0.5 | 0.25-1 | >32 |
| 42a | S |  | <0.008-0.03 | <0.008-0.015 | <0.008 | <0.008 | 1-2 | 0.5-2 | >16 |
| 42b | S |  | 1 | 0.5 | 0.25 | 0.25-0.5 | 2->16 | 1->16 | >16 |
| 47 |  |  | <0.03-0.25 | <0.03-0.125 | <0.03 | <0.03-0.06 | >64 | >64 | >64 |
| rac-GP-1 | | | 0.015-0.06 | <0.008 | <0.008-0.015 | <0.008-0.015 | 0.25-1 | 0.06-0.5 | 0.5-2 |
| Levofloxacin | | | 16-64 | 0.25-8 | 4->64 | 0.125-4 | 0.5-16 | ≤0.03->64 | 0.5-4 |

^aMRSA, methicillin-resistant *S. aureus*, 4 strains; MSSA, methicillin-sensitive *S. aureus*, 4 strains; MRSE, methicillin-resistant *S. epidermidis*, 4 strains; MSSE, methicillin-sensitive *S. epidermidis*, 4 strains; ECO⁺, ESBL-producing *E. coli*, 3 strains; ECO⁻, non-ESBL-producing *E. coli*, 3 strains; and PAE, IMP-4 producing MDR *P. aeruginosa*, 3 strains.

Microsomal Stability and PK Profile of Selected Pyrimido[4,5-*b*]indoles. Based on their *in vitro* antibacterial activities, compounds 18k–m, 18o–p, 31b–c, and 34c were selected to examine their metabolic stability in a liver microsome assay. The results are summarized in Table 6. Although the liver microsomal stability of compounds 18k–m, 18o–p, and 31b–c in humans was acceptable, with the metabolic bioavailability (MF) of 18p reaching 82.2%, the data in rats were poor, and their MFs were all below 40%. Hence, the metabolite identification study of compound 18k was conducted *in vitro* in rat liver microsomes. It was demonstrated that metabolite M5 with demethylation at R5 was the major

metabolite, accounting for 72.85% of the metabolites observed (more details can be found in the Supporting Information), and the methyl group at R5 was considered to be a soft spot.

To improve the metabolic properties of these pyrimidoindoles, CD₃ was exploited in the R5 position of compounds 63b–e, which is a classic strategy to solve PK problems caused by methyl groups.³² The G⁻ activities of these compounds were also evaluated. They maintained superior activity against G⁻ pathogens in accordance with CH₃ analogues, as shown in Table 5. Since the activity of compound 63d was better than that of 63e, the (R)-configuration was preferred for this C-4 moiety. Compounds 63b–d was then tested in liver micro-

Table 6. Microsomal Stability of Selected Compounds

| compd | species | $T_{1/2}^a$ (min) | Cl_{int}^b (mL/min/g protein) | MF ^c (%) |
|-------|---------|-------------------|---------------------------------|---------------------|
| 18k | Rat | 28.3 | 74.3 | 37.4 |
| | Human | 147 | 14.3 | 57.8 |
| 18l | Rat | 17.8 | 118.3 | 27.3 |
| | Human | 38.0 | 55.2 | 26.2 |
| 18m | Rat | 24.9 | 84.4 | 34.5 |
| | Human | 47.5 | 44.3 | 30.7 |
| 18o | Rat | 12.0 | 180.9 | 19.7 |
| | Human | 107 | 19.6 | 50.0 |
| 18p | Rat | 16.7 | 126 | 26.1 |
| | Human | 494 | 4.25 | 82.2 |
| 18r | Rat | 8.3 | 252 | 15.0 |
| | Human | 73.9 | 28.4 | 40.8 |
| 31b | Rat | 11.9 | 176.4 | 20.1 |
| | Human | 57.8 | 36.3 | 35.0 |
| 31c | Rat | 15.2 | 138.4 | 24.3 |
| | Human | 54.7 | 38.4 | 33.8 |
| 34c | Rat | 45.6 | 256.1 | 14.8 |
| | Human | 76.0 | 51.4 | 27.6 |
| 63b | Rat | 32.9 | 63.9 | 41.0 |
| | Human | 105 | 20.0 | 49.6 |
| 63c | Rat | 20.2 | 104 | 30.0 |
| | Human | 208 | 10.1 | 66.0 |
| 63d | Rat | 9.8 | 215 | 17.2 |
| | Human | 179 | 11.7 | 62.6 |

^a $T_{1/2}$: elimination half-life. ^b Cl_{int} : intrinsic body clearance. ^cCalculated metabolic bioavailability.

with an ethyl group at the R5 position was designed in order to further improve the PK properties of **18r**. It was slightly better than **18r** in the PK profile, but the activity was totally lost suggesting that only small groups were tolerated at the R5 position.

In Vivo Efficacy of Compound 18r. Compound **18r** was evaluated for its *in vivo* efficacy after intravenous injection in a neutropenic mouse thigh infection model. The animals were infected by a clinically isolated strain of MDR *A. baumannii* that produces OXA-23. Levofloxacin was tested as a positive control as it was reported that the *in vivo* potency of GP-1 against G⁻ bacteria was worse than levofloxacin.²⁰ As shown in Figure 3, the corresponding log units of cfu reduction under different dosing regimens were used to demonstrate the efficacy. A dose–response trend was observed for compound **18r** (10, 20, and 30 mg/kg), and at 30 mg/kg, **18r** showed

Table 7. *In Vivo* PK Properties of Selected Compounds in Rats after Intravenous Administration^a

| compd | dose (mg/kg) | AUC _{0–∞} (ng·h/mL) | $T_{1/2}$ (h) | MRT (h) | Cl (mL/min/kg) | V_{ss} (L/kg) |
|-------|--------------|------------------------------|---------------|-----------|----------------|-----------------|
| 18k | 4 | 776 ± 44.0 | 3.7 ± 0.8 | 2.8 ± 1.0 | 86.7 ± 4.8 | 14.7 ± 5.9 |
| 18m | 4 | 778 ± 103.9 | 4.7 ± 1.1 | 4.4 ± 1.0 | 86.8 ± 12.4 | 22.5 ± 2.3 |
| 18o | 4 | 836 ± 153 | 9.0 ± 1.7 | 6.8 ± 0.5 | 81.5 ± 14.4 | 33.4 ± 6.9 |
| 18p | 4 | 1513 ± 48 | 5.7 ± 0.5 | 4.7 ± 0.6 | 44.1 ± 1.4 | 12.3 ± 1.1 |
| 31c | 4 | 983 ± 294.5 | 2.7 ± 0.4 | 2.1 ± 0.7 | 71.5 ± 18.4 | 9.3 ± 4.5 |
| 61 | 4 | 517 ± 169 | 6.5 ± 0.4 | 8.3 ± 0.9 | 141 ± 54 | 68.4 ± 19.5 |
| 63c | 5 | 696 ± 93 | 7.2 ± 0.9 | 5.9 ± 0.6 | 121 ± 16 | 43.2 ± 9.1 |
| 63d | 5 | 634 ± 47 | 6.5 ± 0.6 | 5.6 ± 0.1 | 132 ± 9 | 44.5 ± 3.7 |
| 63f | 5 | 1292 ± 84 | 6.7 ± 0.7 | 4.3 ± 0.3 | 64.7 ± 4.4 | 16.7 ± 0.5 |
| 18r | 5 | 1099 ± 134 | 8.5 ± 1.3 | 7.8 ± 1.0 | 76.6 ± 8.9 | 35.7 ± 5.7 |
| 18r | 20 | 5787 ± 258 | 5.9 ± 0.2 | 3.1 ± 0.4 | 57.7 ± 2.5 | 10.8 ± 0.9 |

^aSprague–Dawley rats (male), iv, $n = 3$. All values are represented as the mean ± standard deviation. Abbreviations: AUC, area under the concentration–time curve; $T_{1/2}$, elimination half-life; MRT, mean residence time; CL, clearance; V_{ss} , volume of distribution at the steady state.

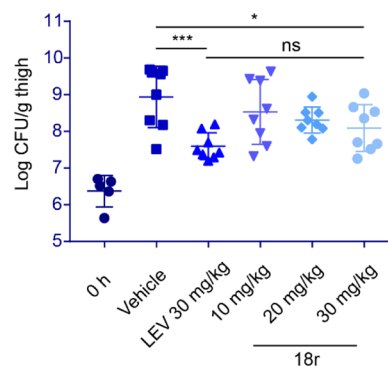


Figure 3. Efficacy study of compound **18r** in a neutropenic mouse thigh model. The figure shows the log unit cfu levels in the OXA-23-producing MDR *A. baumannii* clinical isolate after 2 h of infection with treatment with either vehicle control, levofloxacin (LEV), or compound **18r**. The line for each animal group represents the mean. Statistical significance (two-tailed *t*-test) vs vehicle; one asterisk represents adjusted *p* values 0.01–0.05, and three asterisks represent *p* < 0.0001. In addition, ns represents no significant difference.

bactericidal efficacy comparable to that of levofloxacin at the same dose.

Cytotoxicity of Compounds 18k, 18n, and 18r. Other than the hERG inhibition test, we also identified the safety profile of compounds by cytotoxicity analysis with two mammalian cells (human L02 and HEK-293). Compounds **18k**, **18n**, and **18r** were evaluated (Table 8) and all CC₅₀

Table 8. CC₅₀ of Selected Compounds in L02 Cells and HEK 293 Cells after Incubation for 48 h

| compd | CC ₅₀ (μM; μg/mL ^a) | |
|----------|--|--------------|
| | L02 | HEK 293 |
| 18k | 9.74; 5.07 | 16.96; 8.82 |
| 18n | 6.99; 3.72 | 29.00; 15.53 |
| 18r | 16.04; 8.34 | 19.02; 9.89 |
| rac-GP-1 | 24.03; 10.43 | 21.80; 9.47 |

^aFor better reading, μg/mL values for cytotoxicity are also included.

values were calculated after 48 h incubation. Cytotoxicity of **18k** and **18n** was relatively high against the L02 cell line (CC₅₀ < 10 μM) while that of compounds **18r** and *rac*-GP-1 was modest. As for HEK 293, these compounds displayed a similar effect and all exerted minor cytotoxicity. The cytotoxicity of

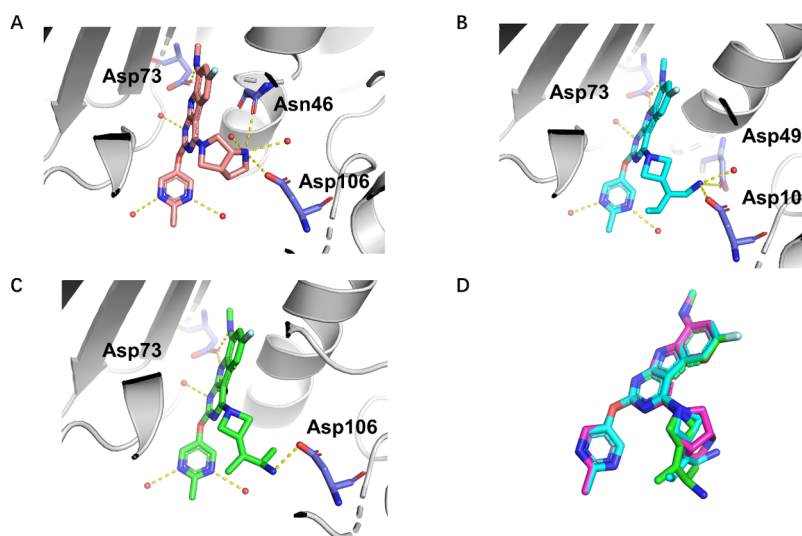


Figure 4. Docking results for compounds **18k** and **18r**. (A) Binding mode of GP-1 in a crystal structure of *E. coli* gyrase (PDB id: 4KFG) was analyzed. (B,C) Binding modes of **18k** (B) and **18r** (C) were predicted using molecular docking. (D) Binding conformation superposition of GP-1, **18k**, and **18r**.

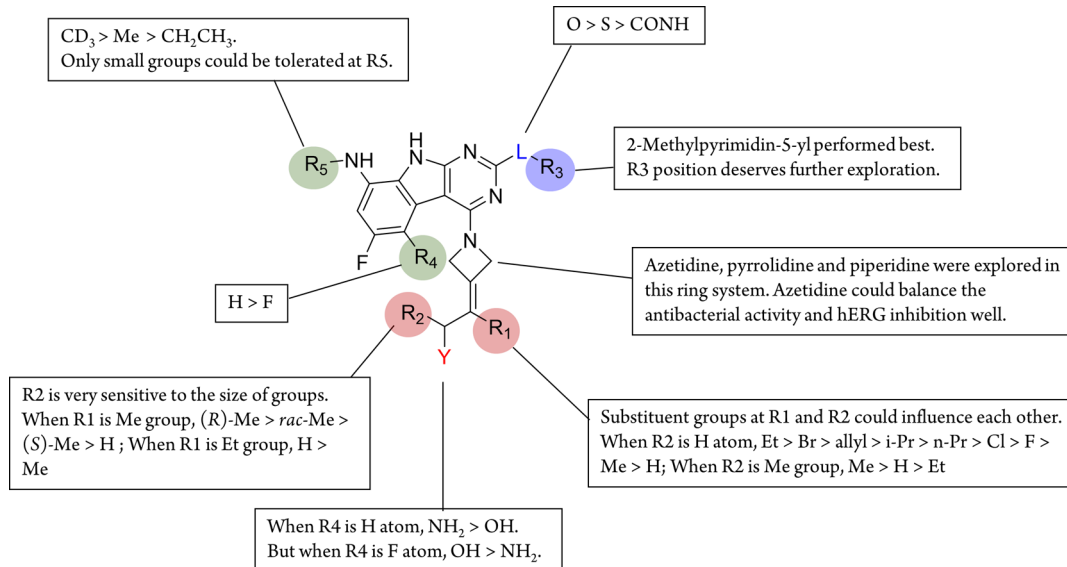


Figure 5. *In Vitro* SAR of Pyrimido[4,5-*b*]indole Derivatives.

compound **18r** (9.89 $\mu\text{g}/\text{mL}$), which was 20–40-fold lower than its antibacterial activity against *A. baumannii*, was comparable with that of *rac*-GP-1. Novel pyrimido[4,5-*b*]indole derivatives did not show superiority over *rac*-GP-1 in this assay.

Binding Mode of Compounds 18k and 18r with *E. coli* Gyrase. In order to gain insights into the binding modes of compounds **18k** and **18r**, we then carried out molecular modeling and docking studies based on the X-ray crystal structure of the DNA gyrase B ATP-binding domain of *E. coli* in complex with GP-1 (PDB code: 4KFG, 1.60 Å resolution).²⁰ The docking results are displayed in Figure 4, which show that compounds **18k** and **18r** bind to GyrB in a similar mode to that of GP-1. Hydrogen bonds between the pyrimido[4,5-*b*]indole tricycle and Asp73 and a water molecule were shared among GP-1, compounds **18k** and **18r**. However, the terminal amine in the C-4 moiety forms a unique hydrogen bond with the carboxylic group of Asp49, while a hydrogen-bond

interaction was observed for GP-1 with Asn46, which may account for the better antibacterial activity of **18k**. Compound **18r**, however, failed to form the same interaction with Asp49, which may explain its slightly reduced activity compared to that of **18k**. It seems that contact with Asp106 is important for the activity of pyrimido[4,5-*b*]indoles, as all three compounds interacted with this residue. More attention should be paid to the interaction with Asp106 in further studies.

CONCLUSIONS

Development of the pyrimido[4,5-*b*]indole derivatives was previously limited due to the hERG liability, poor PK property, and insufficient efficacy *in vivo* against G⁻ bacteria. In this study, based on the pyrimidoindole scaffold of GP-1 and the C-7 moiety of acorofloxacin, novel analogues with varied substitutions at multiple positions were designed and synthesized, and their SARs, hERG inhibition, PK profiles, *in vivo* efficacy as well as cytotoxicity, and binding mode were

studied. A summary of the *in vitro* SAR of these pyrimido[4,5-*b*]indole compounds is presented in Figure 5. Compounds with a unique C-4 moiety consisting of an azetidine ring, an exocyclic double bond, and a terminal amine group demonstrated excellent broad-spectrum antibacterial activity, including a variety of clinical MDR G⁻ pathogens, especially *A. baumannii*. Simultaneously, these compounds successfully evaded hERG K⁺ channel inhibition. A structure–metabolism relationship study led to the discovery of compound **18r**, with an improved *in vivo* PK profile and therapeutic efficacy in a neutropenic mouse thigh infection model. Nevertheless, compound **18r** still displayed minor cytotoxicity as other pyrimido[4,5-*b*]indole derivatives, and the *in vivo* efficacy against MDR *A. baumannii* of this compound is moderate which is probably due to the modest AUC and high clearance.

A broad-spectrum antibacterial agent is of importance to the treatment of MDR bacterial infection in clinical application, but the development of these agents with a novel mechanism or novel target is slow.³³ Compound **18r** as a novel pyrimido[4,5-*b*]indole derivative demonstrated outstanding broad-spectrum activity against both G⁺ and G⁻ pathogens. It provides a substantial foundation for the discovery of a new class of broad-spectrum antibiotic. Based on the excellent lead **18r**, we would carry out more following research on this series to further improve the PK profile, safety, and *in vivo* efficacy against MDR G⁻ bacteria.

EXPERIMENTAL SECTION

Chemistry. All solvents and chemicals were used as purchased without further purification. Inert atmosphere operations were conducted under argon in flame-dried glassware. Room temperature refers to 20–25 °C. The microwave-assisted reactions were carried out in a CEM Discover microwave synthesizer. Intermediates not described below were purchased from commercial vendors and were used as supplied unless stated otherwise. All reaction mixtures were monitored using thin-layer chromatography (TLC) on silica gel F-254 TLC plates. Column chromatography was carried out using silica gel (200–300 mesh). ¹H and ¹³C NMR spectra were recorded on a Bruker 400, a Bruker 500, or a Bruker 600 NMR spectrometer using the solvent residue as the internal standards. Chemical shifts (δ) are reported in parts per million (ppm), and coupling constants (*J*) are reported in hertz (Hz). Electron ionization (EI)-mass spectrometry (MS) images were obtained on a Finnigan MAT95 spectrometer, and electrospray ionization (ESI)-MS images were obtained on a Krats MS 80 mass spectrometer. Purification of all intermediates or final compounds was determined by either column chromatography or preparative reverse-phase high-performance liquid chromatography (HPLC) (SunFire C¹⁸OBD 100 mm × 30 mm; particle size, 5 μ m) with acetonitrile/buffer (0.1 CF₃COOH in water) as the mobile phase. Purity of all final compounds was determined by analytical HPLC (PLATISIL ODS 250 mm × 4.6 mm, particle size 5 μ m) with acetonitrile/buffer (0.1 CF₃COOH in water) as the mobile phase. The ee values were determined using chiral HPLC (CHIRALCEL OD-H column 250 mm × 4.6 mm, particle size 5 μ m or CHIRALPAK IA column 250 mm × 4.6 mm, particle size 5 μ m) with ethanol/*n*-hexane or methanol/ethanol/0.1% diethylamine (DEA) as the mobile phase. A purity of >95% was achieved for all tested compounds. Detailed synthetic procedure and spectral characterization for all intermediates are provided in the Supporting Information.

4-(4-(2-Aminoethylidene)piperidin-1-yl)-6-fluoro-N-methyl-2-((2-methylpyrimidin-5-yl)oxy)-9H-pyrimido[4,5-*b*]indol-8-amine (18a). Intermediate **16a** (144 mg, 563 μ mol) was dissolved in 1-methyl-2-pyrrolidinone (NMP) (5 mL) within a microwave vial. Compound **11** (150 mg, 281 μ mol) and potassium carbonate (K₂CO₃) (117 mg, 845 μ mol) were added into the solution. The vial was capped and heated in a microwave reactor at 100 °C for 3 h.

Afterward, the reaction mixture was cooled to room temperature. The reaction mixture was poured into 15 mL of water and a white precipitate appeared. After filtration and drying, the white solid was redissolved in 2 mL of dichloromethane (DCM), and trifluoroacetic acid (TFA) (2.0 mL, 26.9 mmol) was added. The reaction mixture was allowed to stir at room temperature for 30 min and then evaporated to dryness in vacuo. The residue was redissolved in 20 mL of methanol, and 85% hydrazine hydrate (1.0 mL, 17.4 mmol) was added. After being reheated to reflux for 1 h, the reaction mixture was then concentrated in vacuo and diluted with water (20 mL). The crude solid product was formed during concentration and was filtered and dried. The crude product was purified by chromatography on silica gel with DCM/methanol (10:1) to afford **18a** as a pale-yellow solid (41 mg, 32% yield). ¹H NMR (600 MHz, DMSO-*d*₆): δ 11.81 (s, 1H), 8.73 (s, 2H), 7.82 (s, 3H), 6.66 (d, *J* = 9.5 Hz, 1H), 6.36 (d, *J* = 11.6 Hz, 1H), 5.35 (t, *J* = 6.9 Hz, 1H), 3.65 (d, *J* = 21.1 Hz, 6H), 2.86 (s, 3H), 2.67 (s, 3H), 2.41 (s, 2H), 2.33 (s, 2H). ¹³C NMR (151 MHz, DMSO-*d*₆): δ 163.23, 161.07, 160.52, 159.84, 158.31, 157.98, 157.64, 150.62 (2C), 146.04, 141.89, 136.56, 120.67, 118.52, 115.80, 95.84, 94.19, 92.18, 48.52, 47.92, 35.55, 34.80, 29.67, 27.91, 24.86. MS (ESI) *m/z*: 449.2 (M + H)⁺. High-resolution mass spectrometry (HRMS) (ESI): Anal. Calcd for C₂₃H₂₆FN₈O [(M + H)⁺]: 449.2208. Found: 449.2211.

4-(4-(1-Aminopropan-2-ylidene)piperidin-1-yl)-6-fluoro-N-methyl-2-((2-methylpyrimidin-5-yl)oxy)-9H-pyrimido[4,5-*b*]indol-8-amine (18b). Compound **18b** (40 mg, 58% yield) was prepared from **11** (80 mg, 150 μ mol), **16b** (81 mg, 300 μ mol), K₂CO₃ (62 mg, 451 μ mol), TFA (2.0 mL, 26.9 mmol), and 85% hydrazine hydrate (1.0 mL, 17.4 mmol) in the same manner as described for **18a** but purified by prep-HPLC (solvent A, 0.1% TFA aqueous solution; solvent B, acetonitrile; gradient, 20–80% B). ¹H NMR (500 MHz, DMSO-*d*₆): δ 11.70 (s, 1H), 8.67 (s, 2H), 7.89 (s, 3H), 6.63 (d, *J* = 9.8 Hz, 1H), 6.30 (d, *J* = 12.0 Hz, 1H), 3.65–3.59 (m, 4H), 3.48 (d, *J* = 5.3 Hz, 2H), 2.81 (s, 3H), 2.63 (s, 3H), 2.42 (s, 2H), 2.37 (s, 2H), 1.74 (s, 3H). ¹³C NMR (126 MHz, DMSO-*d*₆): δ 163.79, 161.55, 160.98, 160.57, 159.27, 158.73, 158.18, 151.11 (2C), 146.64, 137.12, 136.25, 121.25, 120.92, 119.27, 96.23, 94.90, 92.74, 48.59, 48.01, 41.04, 30.22, 29.66, 29.41, 25.28, 16.86. MS (ESI) *m/z*: 463.2 (M + H)⁺. HRMS (ESI): Anal. Calcd for C₂₄H₂₈FN₈O [(M + H)⁺]: 463.2375. Found: 463.2365.

4-(4-(2-Amino-1-fluoroethylidene)piperidin-1-yl)-6-fluoro-N-methyl-2-((2-methylpyrimidin-5-yl)oxy)-9H-pyrimido[4,5-*b*]indol-8-amine (18c). Compound **15** (120 mg, 272 μ mol) and triethylamine (83 mg, 817 μ mol) was dissolved in 5 mL of NMP. The BOP reagent (169 mg, 381 μ mol) was added into the solution at 0 °C under an argon atmosphere, and the reaction mixture was stirred for 30 min. Then, intermediate **16c** (155 mg, 564 μ mol) dissolved in 5 mL of NMP was added dropwise to the mixture. The reaction mixture was heated to 50 °C and stirred for 1 h. The mixture was diluted with 20 mL of water and a white solid was precipitated out. The precipitate was obtained after filtration and drying. It was redissolved in 2 mL of DCM, and TFA (2.0 mL, 26.9 mmol) was added. The reaction mixture was allowed to stir at room temperature for 30 min and then evaporated to dryness in vacuo. The residue was redissolved in 20 mL of methanol, and 85% hydrazine hydrate (1.0 mL, 17.4 mmol) was added. After being reheated to reflux for 1 h, the reaction mixture was then concentrated in vacuo and diluted with water (20 mL). The crude solid was product formed during concentration and was filtered and dried. The crude product was purified by chromatography on silica gel with DCM/methanol (10:1) to afford **18c** as a pale-yellow solid (72 mg, 57% yield). ¹H NMR (600 MHz, DMSO-*d*₆): δ 8.74 (s, 2H), 6.66 (dd, *J* = 10.0, 2.0 Hz, 1H), 6.36 (dd, *J* = 12.1, 1.9 Hz, 1H), 5.64 (d, *J* = 4.5 Hz, 1H), 3.71–3.61 (m, 4H), 3.35 (d, *J* = 23.5 Hz, 2H), 2.86 (d, *J* = 4.8 Hz, 3H), 2.67 (d, *J* = 9.8 Hz, 3H), 2.40–2.36 (m, 2H), 2.36–2.31 (m, 2H). ¹³C NMR (151 MHz, DMSO-*d*₆): δ 163.39, 161.25, 160.79, 160.00, 158.47, 157.77, 150.80 (2C), 146.22, 136.70, 120.84, 118.70, 111.44, 95.98, 94.42, 92.30, 48.35, 47.55, 38.32, 29.83, 26.64, 25.02, 24.67. MS (ESI) *m/z*: 467.2 (M + H)⁺. HRMS (ESI): Anal. Calcd for C₂₃H₂₅F₂N₈O [(M + H)⁺]: 467.2114. Found: 467.2128.

(*Z*)-4-(3-(2-Amino-1-fluoroethylidene)pyrrolidin-1-yl)-6-fluoro-*N*-methyl-2-((2-methylpyrimidin-5-yl)oxy)-9*H*-pyrimido[4,5-*b*]indol-8-amine (**18d**). Compound **18d** (33 mg, 21% yield) was prepared from **15** (150 mg, 341 μ mol), **16d** (133 mg, 511 μ mol), BOP reagent (211 mg, 477 μ mol), triethylamine (103 mg, 1.02 mmol), TFA (2.0 mL, 26.9 mmol), and 85% hydrazine hydrate (1.0 mL, 17.4 mmol) in the same manner as described for **18c**. ^1H NMR (400 MHz, DMSO- d_6): δ 8.70 (s, 2H), 7.02 (d, J = 10.9 Hz, 1H), 6.28 (d, J = 11.9 Hz, 1H), 5.54 (s, 1H), 4.49 (s, 2H), 4.00 (t, J = 6.9 Hz, 2H), 3.27 (s, 2H), 2.82 (d, J = 4.4 Hz, 3H), 2.69 (s, 2H), 2.65 (s, 3H). ^{13}C NMR (126 MHz, DMSO- d_6): δ 163.73, 161.40, 160.55, 158.72, 158.34, 157.81, 153.61, 151.21 (2C), 146.65, 136.98, 121.27, 119.32, 113.84, 95.15, 95.00, 92.33, 49.71, 49.20, 30.28, 26.43, 25.45. MS (ESI) m/z : 453.3 (M + H) $^+$. HRMS (ESI): Anal. Calcd for C₂₂H₂₃F₂N₈O [(M + H) $^+$]: 453.1957. Found: 453.1966.

(*E*)-4-(3-(2-Amino-1-fluoroethylidene)pyrrolidin-1-yl)-6-fluoro-*N*-methyl-2-((2-methylpyrimidin-5-yl)oxy)-9*H*-pyrimido[4,5-*b*]indol-8-amine (**18e**). Compound **18e** (45 mg, 50% yield) was prepared from **15** (70 mg, 159 μ mol), **16e** (83 mg, 303 μ mol), BOP reagent (98 mg, 223 μ mol), triethylamine (48 mg, 477 μ mol), TFA (2.0 mL, 26.9 mmol), and 85% hydrazine hydrate (1.0 mL, 17.4 mmol) in the same manner as described for **18c** but purified by prep-HPLC (solvent A, 0.1% TFA aqueous solution; solvent B, acetonitrile; gradient, 20–80% B). ^1H NMR (500 MHz, DMSO- d_6): δ 11.73 (s, 1H), 8.69 (s, 2H), 8.32 (s, 3H), 6.96 (dd, J = 10.9, 1.4 Hz, 1H), 6.30 (dd, J = 11.9, 1.6 Hz, 1H), 4.48 (s, 2H), 4.04 (t, J = 7.0 Hz, 2H), 3.80 (d, J = 20.7 Hz, 2H), 2.83 (s, 3H), 2.77 (t, J = 6.3 Hz, 2H), 2.65 (s, 3H). ^{13}C NMR (126 MHz, DMSO- d_6): δ 163.79, 161.40, 160.60, 158.68, 158.53–158.51, 158.37, 157.88, 151.22 (2C), 146.65, 144.68, 137.06, 121.36, 120.54, 119.25, 95.17, 95.00, 92.43, 49.60, 49.22, 37.48, 30.28, 26.84, 25.45. MS (ESI) m/z : 453.3 (M + H) $^+$. HRMS (ESI): Anal. Calcd for C₂₂H₂₃F₂N₈O [(M + H) $^+$]: 453.1957. Found: 453.1966.

4-(3-(2-Aminoethylidene)azetididin-1-yl)-6-fluoro-*N*-methyl-2-((2-methylpyrimidin-5-yl)oxy)-9*H*-pyrimido[4,5-*b*]indol-8-amine (**18f**). Compound **18f** (97 mg, 82% yield) was prepared from **11** (150 mg, 282 μ mol), **16f** (78 mg, 338 μ mol), K₂CO₃ (117 mg, 845 μ mol), TFA (2.0 mL, 26.9 mmol), and 85% hydrazine hydrate (1.0 mL, 17.4 mmol) in the same manner as described for **18a**. ^1H NMR (500 MHz, DMSO- d_6): δ 8.70 (s, 2H), 6.87 (d, J = 9.1 Hz, 1H), 6.28 (d, J = 12.0 Hz, 1H), 5.67 (d, J = 4.3 Hz, 1H), 5.51 (s, 1H), 5.06 (s, 2H), 4.90 (s, 2H), 3.22 (d, J = 6.3 Hz, 2H), 2.83 (d, J = 4.5 Hz, 3H), 2.65 (s, 3H). ^{13}C NMR (126 MHz, DMSO- d_6): δ 163.72, 161.85, 159.67, 158.86, 157.18, 151.14 (2C), 146.65, 137.03, 130.96, 121.60, 121.21, 118.88, 94.75, 94.37, 92.48, 60.38, 29.86. MS (ESI) m/z : 421.2 (M + H) $^+$. HRMS (ESI): Anal. Calcd for C₂₁H₂₂FN₈O [(M + H) $^+$]: 421.1895. Found: 421.1886.

4-(3-(2-Amino-1-fluoroethylidene)azetididin-1-yl)-6-fluoro-*N*-methyl-2-((2-methylpyrimidin-5-yl)oxy)-9*H*-pyrimido[4,5-*b*]indol-8-amine (**18g**). Compound **18g** (58 mg, 49% yield) was prepared from **15** (120 mg, 272 μ mol), **16g** (101 mg, 409 μ mol), BOP reagent (169 mg, 381 μ mol), triethylamine (83 mg, 817 μ mol), TFA (2.0 mL, 26.9 mmol), and 85% hydrazine hydrate (1.0 mL, 17.4 mmol) in the same manner as described for **18c**. ^1H NMR (600 MHz, DMSO- d_6): δ 8.68 (s, 2H), 6.84 (dd, J = 10.2, 2.0 Hz, 1H), 6.27 (dd, J = 12.1, 2.0 Hz, 1H), 5.50 (d, J = 4.3 Hz, 1H), 5.09 (s, 2H), 4.89 (s, 2H), 3.27 (d, J = 13.6 Hz, 2H), 2.81 (d, J = 4.9 Hz, 3H), 2.63 (s, 3H). ^{13}C NMR (151 MHz, DMSO- d_6): δ 163.35, 161.41, 159.17, 158.58, 156.74, 150.76 (2C), 146.16, 136.53, 120.74 s, 118.32, 118.10, 105.93, 105.77, 94.27, 93.96, 92.16, 56.84, 56.43, 29.81, 25.02, 1.17. MS (ESI) m/z : 439.3 (M + H) $^+$. HRMS (ESI): Anal. Calcd for C₂₁H₂₁F₂N₈O [(M + H) $^+$]: 439.1801. Found: 439.1810.

4-(3-(2-Amino-1-chloroethylidene)azetididin-1-yl)-6-fluoro-*N*-methyl-2-((2-methylpyrimidin-5-yl)oxy)-9*H*-pyrimido[4,5-*b*]indol-8-amine (**18h**). Compound **18h** (73 mg, 49% yield) was prepared from **15** (120 mg, 272 μ mol), **16h** (100 mg, 381 μ mol), BOP reagent (169 mg, 381 μ mol), triethylamine (83 mg, 817 μ mol), TFA (2.0 mL, 26.9 mmol), and 85% hydrazine hydrate (1.0 mL, 17.4 mmol) in the same manner as described for **18c**. ^1H NMR (600 MHz, DMSO- d_6): δ 11.82 (s, 1H), 8.73 (s, 2H), 8.36 (s, 3H), 6.89 (dd, J = 10.0, 1.8 Hz, 1H), 6.33 (dd, J = 12.1, 1.9 Hz, 1H), 5.18 (s, 2H), 4.93 (s, 2H), 3.82

(s, 2H), 2.85 (s, 3H), 2.68 (s, 3H). ^{13}C NMR (151 MHz, DMSO- d_6): δ 163.41, 161.34, 160.20, 159.31, 158.82–158.14, 156.82, 150.71 (2C), 146.14, 136.64, 134.31, 120.88, 118.17, 117.62, 115.48, 94.62, 93.95, 92.32, 59.12, 58.92, 41.12, 29.80, 25.01. MS (ESI) m/z : 455.3 (M + H) $^+$. HRMS (ESI): Anal. Calcd for C₂₁H₂₁ClFN₈O [(M + H) $^+$]: 455.1505. Found: 455.1517.

4-(3-(2-Amino-1-bromoethylidene)azetididin-1-yl)-6-fluoro-*N*-methyl-2-((2-methylpyrimidin-5-yl)oxy)-9*H*-pyrimido[4,5-*b*]indol-8-amine (**18i**). Compound **18i** (63 mg, 46% yield) was prepared from **15** (120 mg, 272 μ mol), **16i** (100 mg, 409 μ mol), BOP reagent (169 mg, 381 μ mol), triethylamine (83 mg, 817 μ mol), TFA (2.0 mL, 26.9 mmol), and 85% hydrazine hydrate (1.0 mL, 17.4 mmol) in the same manner as described for **18c**. ^1H NMR (400 MHz, DMSO- d_6): δ 8.73 (s, 2H), 6.88 (d, J = 9.4 Hz, 1H), 6.31 (d, J = 10.6 Hz, 1H), 5.74 (s, 1H), 5.17 (s, 2H), 4.77 (s, 2H), 3.51 (s, 2H), 2.84 (d, J = 4.6 Hz, 3H), 2.67 (s, 3H). ^{13}C NMR (126 MHz, DMSO- d_6): δ 163.31, 161.31, 160.26, 159.19, 158.42, 156.71, 150.66 (2C), 146.13, 136.58, 129.83, 120.80, 118.23, 94.48, 93.80, 92.12, 61.88–61.10, 60.22, 46.63, 29.73, 24.98. MS (ESI) m/z : 499.2 (M + H) $^+$. HRMS (ESI): Anal. Calcd for C₂₁H₂₁BrFN₈O [(M + H) $^+$]: 499.1000. Found: 499.1011.

4-(4-(1-Aminopropan-2-ylidene)piperidin-1-yl)-6-fluoro-*N*-methyl-2-((2-methylpyrimidin-5-yl)oxy)-9*H*-pyrimido[4,5-*b*]indol-8-amine (**18j**). Compound **18j** (25 mg, 26% yield) was prepared from **11** (120 mg, 225 μ mol), **16j** (109 mg, 451 μ mol), K₂CO₃ (93 mg, 676 μ mol), TFA (2.0 mL, 26.9 mmol), and 85% hydrazine hydrate (1.0 mL, 17.4 mmol) in the same manner as described for **18a** but purified by prep-HPLC (solvent A, 0.1% TFA aqueous solution; solvent B, acetonitrile; gradient, 20–80% B). ^1H NMR (500 MHz, DMSO- d_6): δ 11.71 (s, 1H), 8.68 (s, 2H), 7.98 (s, 3H), 6.90 (d, J = 10.1 Hz, 1H), 6.29 (d, J = 12.1 Hz, 1H), 5.06 (s, 2H), 4.90 (s, 2H), 3.38 (d, J = 4.9 Hz, 2H), 2.81 (s, 3H), 2.64 (s, 3H), 1.68 (s, 3H). ^{13}C NMR (126 MHz, DMSO- d_6): δ 163.80, 161.86, 160.74, 159.74, 158.91, 157.20, 151.12 (2C), 146.62, 136.97, 130.28, 121.64, 121.21, 118.89, 118.79, 94.84, 94.48, 92.63, 59.72, 59.48, 40.68, 30.25, 25.41, 15.69. MS (ESI) m/z : 435.3 (M + H) $^+$. HRMS (ESI): Anal. Calcd for C₂₂H₂₄FN₈O [(M + H) $^+$]: 435.2052. Found: 435.2056.

4-(3-(1-Aminobutan-2-ylidene)azetididin-1-yl)-6-fluoro-*N*-methyl-2-((2-methylpyrimidin-5-yl)oxy)-9*H*-pyrimido[4,5-*b*]indol-8-amine (**18k**). Compound **18k** (31 mg, 24% yield) was prepared from **11** (120 mg, 225 μ mol), **16k** (81 mg, 316 μ mol), K₂CO₃ (93 mg, 676 μ mol), TFA (2.0 mL, 26.9 mmol), and 85% hydrazine hydrate (1.0 mL, 17.4 mmol) in the same manner as described for **18a** but purified by prep-HPLC (solvent A, 0.1% TFA aqueous solution; solvent B, acetonitrile; gradient, 20–80% B). ^1H NMR (500 MHz, DMSO- d_6): δ 11.76 (s, 1H), 8.72 (s, 2H), 7.93 (s, 3H), 6.94 (dd, J = 10.1, 1.8 Hz, 1H), 6.32 (dd, J = 12.1, 1.9 Hz, 1H), 5.13 (s, 2H), 5.01 (s, 2H), 3.43 (d, J = 5.3 Hz, 2H), 2.85 (s, 3H), 2.67 (s, 3H), 2.12 (d, J = 7.5 Hz, 2H), 1.03 (t, J = 7.5 Hz, 3H). ^{13}C NMR (126 MHz, DMSO- d_6): δ 163.81, 161.91, 160.75, 159.82, 158.92, 157.20, 151.15 (2C), 146.64, 137.02, 130.55, 127.13, 121.23, 118.83, 118.29, 94.83, 94.53, 92.64, 59.92, 59.42, 38.26, 30.28, 25.46, 22.69, 12.41. MS (ESI) m/z : 449.2 (M + H) $^+$. HRMS (ESI): Anal. Calcd for C₂₃H₂₆FN₈O [(M + H) $^+$]: 449.2208. Found: 449.2207.

4-(3-(1-Amino-3-methylbutan-2-ylidene)azetididin-1-yl)-6-fluoro-*N*-methyl-2-((2-methylpyrimidin-5-yl)oxy)-9*H*-pyrimido[4,5-*b*]indol-8-amine (**18l**). Compound **18l** (39 mg, 25% yield) was prepared from **15** (120 mg, 272 μ mol), **16l** (130 mg, 490 μ mol), BOP reagent (169 mg, 381 μ mol), triethylamine (83 mg, 817 μ mol), TFA (2.0 mL, 26.9 mmol), and 85% hydrazine hydrate (1.0 mL, 17.4 mmol) in the same manner as described for **18c**. ^1H NMR (500 MHz, DMSO- d_6): δ 11.75 (s, 1H), 8.69 (s, 2H), 7.93 (s, 3H), 6.91 (dd, J = 10.2, 1.9 Hz, 1H), 6.30 (dd, J = 12.2, 2.0 Hz, 1H), 5.10 (d, J = 45.9 Hz, 4H), 4.20 (d, J = 5.8 Hz, 1H), 3.39 (d, J = 5.3 Hz, 2H), 2.83 (s, 3H), 2.65 (s, 3H), 1.06 (d, J = 6.9 Hz, 6H). ^{13}C NMR (126 MHz, DMSO- d_6): δ 163.33, 161.43, 160.25, 159.25, 158.42, 158.16, 156.69, 150.67 (2C), 146.14, 136.53, 130.58, 129.92, 120.74, 118.33, 115.40, 94.32, 94.02, 92.13, 59.97, 59.29, 37.50, 29.90, 29.77, 24.95, 20.53 (2C). MS (ESI) m/z : 463.2 (M + H) $^+$. HRMS (ESI): Anal. Calcd for C₂₄H₂₈FN₈O [(M + H) $^+$]: 463.2365. Found: 463.2365.

4-(3-(1-Aminopentan-2-ylidene)azetid-1-yl)-6-fluoro-N-methyl-2-((2-methylpyrimidin-5-yl)oxy)-9H-pyrimido[4,5-b]indol-8-amine (**18m**). Compound **18m** (61 mg, 35% yield) was prepared from **11** (200 mg, 376 μ mol), **16m** (183 mg, 676 μ mol), K_2CO_3 (156 mg, 1.13 mmol), TFA (2.0 mL, 26.9 mmol), and 85% hydrazine hydrate (1.0 mL, 17.4 mmol) in the same manner as described for **18a**. 1H NMR (600 MHz, $DMSO-d_6$): δ 8.72 (s, 2H), 6.92 (d, J = 10.3 Hz, 1H), 6.30 (d, J = 12.0 Hz, 1H), 5.60 (s, 1H), 5.12 (s, 2H), 4.93 (s, 2H), 3.15 (d, J = 9.6 Hz, 2H), 2.84 (s, 3H), 2.68 (s, 3H), 2.00 (s, 2H), 1.43 (d, J = 7.3 Hz, 2H), 0.90 (t, J = 7.1 Hz, 3H). ^{13}C NMR (151 MHz, $DMSO-d_6$): δ 163.31, 161.52, 159.28, 158.54, 156.69, 150.76 (2C), 146.22, 136.49, 133.26, 122.38, 120.68, 118.52, 94.25, 94.05, 92.05, 59.85, 59.33, 41.98, 31.32, 31.17, 29.83, 25.02, 20.32, 13.95. MS (ESI) m/z : 463.2 (M + H) $^+$. HRMS (ESI): Anal. Calcd for $C_{24}H_{28}FN_8O$ [(M + H) $^+$]: 463.2365. Found: 463.2353.

4-(3-(1-Aminopent-4-en-2-ylidene)azetid-1-yl)-6-fluoro-N-methyl-2-((2-methylpyrimidin-5-yl)oxy)-9H-pyrimido[4,5-b]indol-8-amine (**18n**). Intermediate **16n** (154 mg, 575 μ mol) was dissolved in NMP (5 mL) within a microwave vial. Compound **11** (170 mg, 319 μ mol) and K_2CO_3 (132 mg, 958 μ mol) were added into the solution. The vial was capped and heated in a microwave reactor at 100 $^\circ C$ for 3 h. Afterward, the reaction mixture was cooled to room temperature. The reaction mixture was poured into 15 mL of water and a white precipitate appeared. After filtration and drying, the white solid was redissolved in 2 mL of DCM, and TFA (2.0 mL, 26.9 mmol) was added. The reaction mixture was allowed to stir at room temperature for 30 min and then evaporated to dryness in vacuo. The residue was redissolved in 10 mL of ethanol and 2 mL of 27–32% methylamine ethanol solution was added. After being reheated to 40 $^\circ C$ and stirred for 1 h, the reaction mixture was then concentrated in vacuo. The residue was purified by chromatography on silica gel with DCM/methanol (10:1) to afford **18a** as a pale-yellow solid (44 mg, 30% yield). 1H NMR (500 MHz, $DMSO-d_6$): δ 8.72 (s, 2H), 6.91 (dd, J = 10.2, 1.6 Hz, 1H), 6.36–6.19 (m, 1H), 5.91–5.77 (m, 1H), 5.58 (d, J = 4.2 Hz, 1H), 5.12 (d, J = 15.4 Hz, 3H), 5.03 (d, J = 10.0 Hz, 1H), 4.92 (s, 2H), 3.14 (s, 2H), 2.85 (d, J = 4.7 Hz, 3H), 2.79 (d, J = 6.5 Hz, 2H), 2.67 (s, 3H). ^{13}C NMR (126 MHz, $DMSO-d_6$): δ 163.74, 161.94, 159.65, 158.85, 157.15, 151.18 (2C), 146.66, 136.97, 136.06, 131.22, 124.42, 121.15, 118.94, 116.51, 94.70, 94.45, 92.48, 60.41, 59.80, 42.65, 34.38, 30.26, 25.46. MS (ESI) m/z : 461.4 (M + H) $^+$. HRMS (ESI): Anal. Calcd for $C_{24}H_{26}FN_8O$ [(M + H) $^+$]: 461.2208. Found: 461.2219.

4-(3-(2-Aminopropylidene)azetid-1-yl)-6-fluoro-N-methyl-2-((2-methylpyrimidin-5-yl)oxy)-9H-pyrimido[4,5-b]indol-8-amine (**18o**). Compound **18o** (190 mg, 38% yield) was prepared from **11** (500 mg, 939 μ mol), **16o** (341 mg, 1.41 mmol), K_2CO_3 (389 mg, 2.82 mmol), TFA (4.0 mL, 53.9 mmol), and 85% hydrazine hydrate (1.0 mL, 17.4 mmol) in the same manner as described for **18k**. 1H NMR (400 MHz, $DMSO-d_6$): δ 11.79 (s, 1H), 8.72 (s, 2H), 7.98 (s, 3H), 6.92 (dd, J = 10.2, 1.8 Hz, 1H), 6.32 (dd, J = 12.2, 2.0 Hz, 1H), 5.50 (d, J = 9.0 Hz, 1H), 5.15 (s, 2H), 4.96 (s, 2H), 3.91 (s, 1H), 2.85 (s, 3H), 2.67 (s, 3H), 1.30 (d, J = 6.6 Hz, 3H). ^{13}C NMR (126 MHz, $DMSO-d_6$): δ 163.25, 161.31, 160.18, 159.20, 158.14, 156.66, 150.61 (2C), 146.05, 136.46, 134.71, 120.66, 119.70, 118.22, 115.24, 94.28, 93.89, 92.09, 59.83, 59.49, 45.17, 29.71, 24.91, 18.85. MS (ESI) m/z : 435.3 (M + H) $^+$. HRMS (ESI): Anal. Calcd for $C_{22}H_{24}FN_8O$ [(M + H) $^+$]: 435.2052. Found: 435.2061.

4-(3-(3-Aminobutan-2-ylidene)azetid-1-yl)-6-fluoro-N-methyl-2-((2-methylpyrimidin-5-yl)oxy)-9H-pyrimido[4,5-b]indol-8-amine (**18p**). Compound **18p** (105 mg, 34% yield) was prepared from **11** (290 mg, 545 μ mol), **16p** (195 mg, 762 μ mol), K_2CO_3 (225.78 mg, 1.63 mmol), TFA (2.0 mL, 26.9 mmol), and 85% hydrazine hydrate (1.0 mL, 17.4 mmol) in the same manner as described for **18k**. 1H NMR (400 MHz, $DMSO-d_6$): δ 11.78 (s, 1H), 8.72 (s, 2H), 8.03 (s, 3H), 6.95 (dd, J = 10.2, 2.0 Hz, 1H), 6.32 (dd, J = 12.2, 2.1 Hz, 1H), 5.13 (s, 2H), 4.93 (s, 2H), 4.00–3.90 (m, 1H), 2.85 (s, 3H), 2.67 (s, 3H), 1.65 (s, 3H), 1.29 (d, J = 6.8 Hz, 3H). ^{13}C NMR (126 MHz, $DMSO-d_6$): δ 163.81, 161.91, 160.75, 159.79, 159.09–158.38, 157.21, 151.15 (2C), 146.64, 137.01, 128.77, 125.29, 121.22, 118.84, 115.72, 94.82, 94.54, 92.64, 59.73, 59.56, 47.76, 30.28, 25.46, 17.45, 11.88.

MS (ESI) m/z : 448.4 (M + H) $^+$. HRMS (ESI): Anal. Calcd for $C_{23}H_{26}FN_8O$ [(M + H) $^+$]: 449.2208. Found: 449.2199.

4-(3-(2-Aminopentan-3-ylidene)azetid-1-yl)-6-fluoro-N-methyl-2-((2-methylpyrimidin-5-yl)oxy)-9H-pyrimido[4,5-b]indol-8-amine (**18q**). Compound **18q** (12 mg, 9% yield) was prepared from **11** (150 mg, 282 μ mol), **16q** (107 mg, 394 μ mol), K_2CO_3 (117 mg, 845 μ mol), TFA (2.0 mL, 26.9 mmol), and 85% hydrazine hydrate (1.0 mL, 17.4 mmol) in the same manner as described for **18a**. 1H NMR (500 MHz, $DMSO-d_6$): δ 8.70 (s, 2H), 6.90 (d, J = 8.8 Hz, 1H), 6.28 (d, J = 10.9 Hz, 1H), 5.52 (s, 1H), 5.09 (s, 2H), 4.90 (s, 2H), 3.56 (d, J = 22.3 Hz, 1H), 2.83 (d, J = 3.8 Hz, 3H), 2.66 (s, 3H), 2.09–1.87 (m, 2H), 1.36 (ddd, J = 63.2, 27.3, 14.0 Hz, 3H), 0.88 (t, J = 7.2 Hz, 3H). ^{13}C NMR (126 MHz, $DMSO-d_6$): δ 165.15, 163.36, 161.12, 160.25, 158.57, 152.59 (2C), 148.09, 138.36, 134.94, 124.45, 122.56, 120.38, 96.14, 95.90d, (J = 26.1 Hz), 93.90, 61.74, 61.17, 43.75, 33.04, 31.69, 26.87, 22.17, 15.80. MS (ESI) m/z : 463.5 (M + H) $^+$. HRMS (ESI): Anal. Calcd for $C_{24}H_{28}FN_8O$ [(M + H) $^+$]: 463.2365. Found: 463.2365.

(R)-4-(3-(3-Aminobutan-2-ylidene)azetid-1-yl)-6-fluoro-N-methyl-2-((2-methylpyrimidin-5-yl)oxy)-9H-pyrimido[4,5-b]indol-8-amine (**18r**). Compound **18r** (97 mg, 35% yield) was prepared from **11** (320 mg, 601 μ mol), **16r** (231 mg, 901 μ mol), K_2CO_3 (249 mg, 1.80 mmol), TFA (2.0 mL, 26.9 mmol), and 85% hydrazine hydrate (1.0 mL, 17.4 mmol) in the same manner as described for **18a**. 1H NMR (500 MHz, $DMSO-d_6$): δ 8.72 (s, 2H), 6.92 (d, J = 9.7 Hz, 1H), 6.30 (d, J = 11.6 Hz, 1H), 5.52 (s, 1H), 5.06 (s, 2H), 4.87 (s, 2H), 3.50 (d, J = 6.3 Hz, 1H), 2.85 (d, J = 4.4 Hz, 3H), 2.67 (s, 3H), 1.55 (s, 3H), 1.07 (d, J = 6.4 Hz, 3H). ^{13}C NMR (126 MHz, $DMSO-d_6$): δ 163.74, 161.95, 160.67, 159.67, 158.84, 157.17, 151.19 (2C), 146.67, 136.89, 133.32, 121.09, 118.99, 94.61, 94.41, 92.49, 60.63–60.21, 59.95, 48.88, 30.28, 25.47 s, 21.90, 12.41. MS (ESI) m/z : 449.2 (M + H) $^+$. HRMS (ESI): Anal. Calcd for $C_{23}H_{26}FN_8O$ [(M + H) $^+$]: 449.2208. Found: 449.2210. The ee value was 94.2%. Chiral HPLC retention time 32.95 min; column: CHIRALPAK IA column (250 mm \times 4.6 mm, 5 μ m); column temperature 30 $^\circ C$; flow rate 0.5 mL/min; detection UV 254 nm; mobile phase: solvent A (80%) = methanol + 0.1% DEA, solvent B (20%) = ethanol + 0.1% DEA; total run time 40 min.

4-(3-(1-Aminobutan-2-ylidene)azetid-1-yl)-6-fluoro-N-methyl-2-(methylsulfonyl)-9H-pyrimido[4,5-b]indol-8-amine (**20**). Compound **19** (100 mg, 154 μ mol) was dissolved in 2 mL of DCM, and TFA (2.0 mL, 26.9 mmol) was added. The reaction mixture was allowed to stir at room temperature for 30 min and then evaporated to dryness in vacuo. The residue was redissolved in 20 mL of methanol, and 85% hydrazine hydrate (1.0 mL, 17.4 mmol) was added. After being reheated to reflux for 1 h, the reaction mixture was then concentrated in vacuo and diluted with water (20 mL). The crude solid product was formed during concentration and was filtered and dried. The crude product was purified by chromatography on silica gel with DCM/methanol (10:1) to afford **20** as a pale-yellow solid (25 mg, 39% yield). 1H NMR (500 MHz, $DMSO-d_6$): δ 12.26 (s, 1H), 7.02 (d, J = 8.5 Hz, 1H), 6.44–6.41 (m, 1H), 5.21 (s, 2H), 5.12 (s, 2H), 3.43 (d, J = 4.8 Hz, 2H), 3.35 (d, J = 4.6 Hz, 3H), 2.88 (d, J = 2.0 Hz, 3H), 2.12 (q, J = 7.2 Hz, 2H), 1.01 (dd, J = 13.1, 7.4 Hz, 3H). ^{13}C NMR (126 MHz, $DMSO-d_6$): δ 161.09, 159.13, 158.40, 158.37–157.93, 154.46, 137.60, 134.98, 130.23, 127.33, 122.71, 118.18, 98.72, 94.85, 93.85, 53.93, 53.64, 38.23, 36.18, 30.24 (s), 22.71, 12.44. MS (ESI) m/z : 419.1 (M + H) $^+$. HRMS (ESI): Anal. Calcd for $C_{19}H_{24}FN_6O_2S$ [(M + H) $^+$]: 419.1660. Found: 419.1666.

4-(3-(1-Aminobutan-2-ylidene)azetid-1-yl)-6-fluoro-8-(methylamino)-9H-pyrimido[4,5-b]indole-2-carbonitrile (**22**). Compound **21** (500 mg, 839 μ mol) was dissolved in 20 mL of methanol, and 85% hydrazine hydrate (1.0 mL, 17.4 mmol) was added. After being heated to reflux for 1 h, the reaction mixture was then concentrated in vacuo and diluted with water (20 mL). A white solid was formed during concentration and was filtered and dried. The white solid was redissolved in 2 mL of DCM, and TFA (2.0 mL, 26.9 mmol) was added. The reaction mixture was allowed to stir at room temperature for 30 min and then evaporated to dryness in vacuo. The residue was purified by chromatography on silica gel with DCM/methanol (10:1)

to afford **22** as a pale-yellow solid (36 mg, 12% yield). ¹H NMR (400 MHz, CD₃OD, SPE): δ 7.30 (d, *J* = 9.3 Hz, 1H), 6.45 (d, *J* = 11.6 Hz, 1H), 4.40 (s, 2H), 3.90 (s, 2H), 3.86 (s, 2H), 2.98 (s, 3H), 2.49 (q, *J* = 7.4 Hz, 2H), 1.14 (t, *J* = 7.6 Hz, 3H). ¹³C NMR (126 MHz, DMSO-*d*₆): δ 160.89, 159.05, 157.90, 153.96, 138.51, 137.57, 134.91, 122.67, 122.14, 117.60, 99.17, 94.76, 93.86, 60.69, 60.37, 42.10, 30.19, 22.90, 12.74. MS (ESI) *m/z*: 366.1 (M + H)⁺. HRMS (ESI): Anal. Calcd for C₁₉H₂₁FN₇ [(M + H)⁺]: 366.1873. Found: 366.1872.

4-(3-(1-Aminobutan-2-ylidene)azetid-1-yl)-6-fluoro-N⁸-methyl-9H-pyrimido[4,5-*b*]indole-2,8-diamine (26). Compound **26** (75 mg, 62% yield) was prepared from **24** (150 mg, 256 μmol), TFA (2.0 mL, 26.9 mmol), and 85% hydrazine hydrate (1.0 mL, 17.4 mmol) in the same manner as described for **19** but purified by prep-HPLC (solvent A, 0.1% TFA aqueous solution; solvent B, acetonitrile; gradient, 20–80% B). ¹H NMR (500 MHz, DMSO-*d*₆): δ 11.64 (s, 1H), 8.00 (s, 3H), 6.83 (dd, *J* = 10.2, 1.6 Hz, 1H), 6.25 (dd, *J* = 12.2, 1.8 Hz, 1H), 5.20 (s, 2H), 5.06 (s, 2H), 3.40 (s, 3H), 2.82 (s, 3H), 2.10 (q, *J* = 7.3 Hz, 2H), 1.00 (t, *J* = 7.5 Hz, 3H). ¹³C NMR (126 MHz, DMSO-*d*₆): δ 160.72, 158.89, 158.58, 158.32, 158.04, 136.87, 127.05, 119.76, 119.61, 118.40, 116.02, 93.68, 91.96, 90.65, 60.34, 59.82, 37.94, 29.78, 22.46, 12.02. MS (ESI) *m/z*: 356.1 (M + H)⁺. HRMS (ESI): Anal. Calcd for C₁₈H₂₃FN₇ [(M + H)⁺]: 356.1993. Found: 356.2001.

N-(4-(3-(1-Aminobutan-2-ylidene)azetid-1-yl)-6-fluoro-8-(methylamino)-9H-pyrimido[4,5-*b*]indol-2-yl)methanesulfonamide (27). Compound **27** (35 mg, 33% yield) was prepared from **25** (130 mg, 196 μmol), TFA (2.0 mL, 26.9 mmol), and 85% hydrazine hydrate (1.0 mL, 17.4 mmol) in the same manner as described for **26**. ¹H NMR (500 MHz, DMSO-*d*₆): δ 11.44 (s, 1H), 9.21 (s, 2H), 7.45–7.30 (m, 2H), 6.26 (d, *J* = 11.9 Hz, 1H), 4.29 (s, 2H), 3.97 (s, 2H), 3.92 (s, 2H), 3.36 (s, 3H), 2.83 (s, 3H), 2.31 (d, *J* = 7.2 Hz, 2H), 0.99 (t, *J* = 7.4 Hz, 3H). ¹³C NMR (126 MHz, DMSO-*d*₆): δ 160.33, 158.77–157.93, 156.74, 155.36, 154.62, 136.29, 133.48, 127.85, 119.84, 118.93, 115.49, 93.22, 92.60, 91.75, 53.31, 53.12, 41.38, 35.32, 29.68, 18.56, 12.32. MS (ESI) *m/z*: 434.2 (M + H)⁺. HRMS (ESI): Anal. Calcd for C₁₉H₂₅FN₇O₂S [(M + H)⁺]: 434.1769. Found: 434.1768.

4-(3-(1-Aminobutan-2-ylidene)azetid-1-yl)-2-((5-cyclopropylpyrimidin-2-yl)oxy)-6-fluoro-N-methyl-9H-pyrimido[4,5-*b*]indol-8-amine (31a). Compound **31a** (105 mg, 34% yield) was prepared from **29a** (250 mg, 428 μmol), **16k** (164 mg, 641 μmol), K₂CO₃ (177 mg, 1.28 mmol), TFA (2.0 mL, 26.9 mmol), and 85% hydrazine hydrate (1.0 mL, 17.4 mmol) in the same manner as described for **18k**. ¹H NMR (500 MHz, DMSO-*d*₆): δ 8.66 (s, 2H), 6.92 (dd, *J* = 10.3, 2.1 Hz, 1H), 6.30 (dd, *J* = 12.2, 2.1 Hz, 1H), 5.59 (d, *J* = 4.3 Hz, 1H), 5.09 (s, 2H), 4.95 (s, 2H), 3.18 (s, 2H), 2.85 (d, *J* = 4.8 Hz, 3H), 2.31–2.22 (m, 1H), 2.04 (dd, *J* = 15.1, 7.5 Hz, 2H), 1.07 (dt, *J* = 8.0, 2.9 Hz, 2H), 1.04–0.97 (m, 5H). ¹³C NMR (126 MHz, DMSO-*d*₆): δ 167.41, 162.03, 159.69, 158.84, 157.15, 151.20 (2C), 146.49, 136.97, 134.27, 123.07, 121.14, 118.91, 94.66, 94.47, 92.46, 60.31, 59.63, 41.79, 30.26, 22.86, 17.95, 12.72, 10.83 (2C). MS (ESI) *m/z*: 475.3 (M + H)⁺. HRMS (ESI): Anal. Calcd for C₂₅H₂₈FN₈O [(M + H)⁺]: 475.2365. Found: 475.2374.

5-((4-(3-(1-Aminobutan-2-ylidene)azetid-1-yl)-6-fluoro-8-(methylamino)-9H-pyrimido[4,5-*b*]indol-2-yl)oxy)pyrimidin-2-yl)methanol (31b). Intermediate **10** (200 mg, 423.27 μmol) was dissolved in NMP (5 mL) within a microwave vial. Compound **28b** (117 mg, 931.20 μmol) and K₂CO₃ (176 mg, 1.27 mmol) were added into the solution. The vial was capped and heated in a microwave reactor at 100 °C for 3 h. After that, compound **16k** (152 mg, 592.58 μmol) was added into the solution. The vial was capped and reheated again in the microwave reactor at 100 °C for 3 h. Afterward, the reaction mixture was cooled to room temperature. The reaction mixture was poured into 15 mL of water and a white precipitate appeared. After filtration and drying, the white solid was redissolved in 2 mL of DCM, and TFA (2.0 mL, 26.9 mmol) was added. The reaction mixture was allowed to stir at room temperature for 30 min and then evaporated to dryness in vacuo. The residue was redissolved in 20 mL of methanol, and 85% hydrazine hydrate (1.0 mL, 17.4 mmol) was added. After being reheated to reflux for 1 h, the reaction

mixture was then concentrated in vacuo and diluted with water (20 mL). The crude solid product was formed during concentration and was filtered and dried. The crude product was purified by chromatography on silica gel with DCM/methanol (10:1) to afford **31b** as a pale-yellow solid (47 mg, 24% yield). ¹H NMR (500 MHz, DMSO-*d*₆): δ 8.80 (s, 2H), 6.91 (d, *J* = 9.7 Hz, 1H), 6.29 (d, *J* = 11.8 Hz, 1H), 5.54 (s, 1H), 5.09 (s, 2H), 4.95 (s, 2H), 4.65 (s, 2H), 3.24 (s, 2H), 2.83 (d, *J* = 3.9 Hz, 3H), 2.05 (d, *J* = 7.2 Hz, 2H), 0.99 (t, *J* = 7.4 Hz, 3H). ¹³C NMR (126 MHz, DMSO-*d*₆): δ 165.23, 161.41, 159.21, 158.37, 156.63, 150.74 (2C), 146.75, 136.48, 131.65, 124.78, 120.69, 118.41, 94.26, 94.01, 92.04, 64.53, 59.74, 59.12, 29.77, 29.00, 22.30, 12.14. MS (ESI) *m/z*: 465.3 (M + H)⁺. HRMS (ESI): Anal. Calcd for C₂₃H₂₆FN₈O₂ [(M + H)⁺]: 465.2157. Found: 465.2157.

1-(5-((4-(3-(1-Aminobutan-2-ylidene)azetid-1-yl)-6-fluoro-8-(methylamino)-9H-pyrimido[4,5-*b*]indol-2-yl)oxy)pyrimidin-2-yl)ethan-1-ol (31c). Compound **31c** (39 mg, 19% yield) was prepared from **10** (200 mg, 423 μmol), **28b** (131 mg, 931 μmol), **16k** (152 mg, 593 μmol), K₂CO₃ (176 mg, 1.27 mmol), TFA (2.0 mL, 26.9 mmol), and 85% hydrazine hydrate (1.0 mL, 17.4 mmol) in the same manner as described for **31b**. ¹H NMR (500 MHz, DMSO-*d*₆): δ 8.80 (s, 2H), 6.89 (dd, *J* = 10.2, 1.8 Hz, 1H), 6.27 (dd, *J* = 12.1, 1.7 Hz, 1H), 5.48 (d, *J* = 4.1 Hz, 1H), 5.06 (s, 2H), 4.91 (s, 2H), 4.84 (q, *J* = 6.5 Hz, 1H), 3.11 (s, 2H), 2.82 (d, *J* = 4.5 Hz, 3H), 2.00 (q, *J* = 7.3 Hz, 2H), 1.45 (d, *J* = 6.6 Hz, 3H), 0.97 (t, *J* = 7.6 Hz, 3H). ¹³C NMR (126 MHz, DMSO-*d*₆): δ 168.47, 161.94, 159.62, 158.83, 157.08, 151.24 (2C), 147.21, 136.92, 135.50, 121.75, 121.14, 118.96, 94.71, 94.50, 94.40, 92.48, 70.08, 60.33, 59.68, 42.39, 30.27, 23.26, 22.86, 12.77. MS (ESI) *m/z*: 479.2 (M + H)⁺. HRMS (ESI): Anal. Calcd for C₂₄H₂₈FN₈O₂ [(M + H)⁺]: 479.2314. Found: 479.2319.

2-(5-((4-(3-(1-Aminobutan-2-ylidene)azetid-1-yl)-6-fluoro-8-(methylamino)-9H-pyrimido[4,5-*b*]indol-2-yl)oxy)pyrimidin-2-yl)propan-2-ol (31d). Compound **31d** (42 mg, 20% yield) was prepared from **10** (200 mg, 423 μmol), **28d** (143 mg, 931 μmol), **16k** (152 mg, 593 μmol), K₂CO₃ (176 mg, 1.27 mmol), TFA (2.0 mL, 26.9 mmol), and 85% hydrazine hydrate (1.0 mL, 17.4 mmol) in the same manner as described for **31b**. ¹H NMR (500 MHz, DMSO-*d*₆): δ 8.83 (s, 2H), 6.94 (d, *J* = 9.6 Hz, 1H), 6.32 (d, *J* = 11.7 Hz, 1H), 5.58 (s, 1H), 5.15 (s, 2H), 4.99 (s, 2H), 3.34 (s, 2H), 2.85 (d, *J* = 3.8 Hz, 3H), 2.10 (d, *J* = 6.9 Hz, 2H), 1.56 (s, 6H), 1.02 (t, *J* = 7.3 Hz, 3H). ¹³C NMR (126 MHz, DMSO-*d*₆): δ 170.03, 161.33, 159.22, 158.32, 156.51, 150.35 (2C), 146.27, 136.49, 129.52, 129.03, 120.62, 118.32, 94.29, 93.90, 92.00, 72.53, 59.52, 58.91 (s), 31.03, 29.66, 28.91, 22.20, 11.92. MS (ESI) *m/z*: 493.3 (M + H)⁺. HRMS (ESI): Anal. Calcd for C₂₅H₃₀FN₈O₂ [(M + H)⁺]: 493.2470. Found: 493.2482.

6-((4-(3-(1-Aminobutan-2-ylidene)azetid-1-yl)-6-fluoro-8-(methylamino)-9H-pyrimido[4,5-*b*]indol-2-yl)oxy)isoindolin-1-one (31e). Compound **31e** (37 mg, 15% yield) was prepared from **10** (200 mg, 423 μmol), **28e** (139 mg, 931 μmol), **16k** (152 mg, 593 μmol), K₂CO₃ (176 mg, 1.27 mmol), TFA (2.0 mL, 26.9 mmol), and 85% hydrazine hydrate (1.0 mL, 17.4 mmol) in the same manner as described for **31b** but purified by prep-HPLC (solvent A, 0.1% TFA aqueous solution; solvent B, acetonitrile; gradient, 20–80% B). ¹H NMR (500 MHz, DMSO-*d*₆): δ 11.74 (s, 1H), 8.66 (s, 1H), 7.97 (s, 3H), 7.63 (d, *J* = 8.0 Hz, 1H), 7.49–7.40 (m, 2H), 6.94 (d, *J* = 9.8 Hz, 1H), 6.31 (d, *J* = 12.0 Hz, 1H), 5.15 (s, 2H), 5.01 (s, 2H), 4.42 (s, 2H), 3.43 (d, *J* = 4.4 Hz, 2H), 2.84 (s, 3H), 2.12 (d, *J* = 7.2 Hz, 2H), 1.03 (t, *J* = 7.5 Hz, 3H). ¹³C NMR (126 MHz, DMSO-*d*₆): δ 169.86, 162.67, 160.70, 160.13, 158.86, 158.79–158.31, 157.44, 153.54, 140.65, 136.94, 134.35, 130.80, 127.03, 125.75, 125.15, 122.19, 118.87, 116.27, 94.64, 94.44, 92.52, 59.97, 59.41, 45.17, 38.29, 30.29, 22.71, 12.41. MS (ESI) *m/z*: 488.3 (M + H)⁺. HRMS (ESI): Anal. Calcd for C₂₆H₂₇FN₇O₂ [(M + H)⁺]: 488.2205. Found: 488.2202.

1-(1-(6-Fluoro-8-(methylamino)-2-((2-methylpyrimidin-5-yl)oxy)-9H-pyrimido[4,5-*b*]indol-4-yl)azetid-3-ylidene)propan-2-ol (34a). Intermediate **32a** (80 mg, 703 μmol) was dissolved in NMP (5 mL) within a microwave vial. Compound **11** (130 mg, 244 μmol) and K₂CO₃ (156 mg, 1.13 mmol) were added into the solution. The vial was capped and heated in a microwave reactor at 100 °C for 2 h. Afterward, the reaction mixture was cooled to room temperature. The reaction mixture was poured into 15 mL of water and a white

precipitate appeared. After filtration and drying, the white solid was redissolved in TFA (2.0 mL, 26.9 mmol). The reaction mixture was allowed to stir at room temperature for 2 min and then evaporated to dryness in vacuo. The residue was adjusted to pH ~8 by saturated solution of sodium bicarbonate. The mixture was extracted with ethyl acetate and the organic phase was washed with water and brine, dried over anhydrous sodium sulfate (Na_2SO_4), and filtered, and the filtrate was concentrated in vacuo. The residue was purified by chromatography on silica gel with DCM/methanol (10:1) to afford **34a** as a white solid (32 mg, 30% yield). ^1H NMR (500 MHz, $\text{DMSO}-d_6$): δ 11.69 (s, 1H), 8.72 (s, 2H), 6.88 (dd, $J = 10.1, 1.3$ Hz, 1H), 6.31 (d, $J = 10.8$ Hz, 1H), 5.54 (d, $J = 4.4$ Hz, 1H), 5.49–5.43 (m, 1H), 5.09 (s, 2H), 4.92 (s, 2H), 4.79 (d, $J = 4.4$ Hz, 1H), 4.27 (d, $J = 5.4$ Hz, 1H), 2.85 (d, $J = 4.8$ Hz, 3H), 2.67 (s, 3H), 1.17 (d, $J = 6.4$ Hz, 3H). ^{13}C NMR (126 MHz, $\text{DMSO}-d_6$): δ 163.74, 161.91, 159.67, 158.84, 157.20, 151.19 (2C), 146.65, 136.97, 128.16, 127.37, 121.15, 118.92, 94.73, 94.40, 92.52, 64.96, 60.45, 30.27, 25.46, 24.08. MS (ESI) m/z : 434.3 (M – H) $^-$. HRMS (ESI): Anal. Calcd for $\text{C}_{22}\text{H}_{21}\text{FN}_7\text{O}_2$ [(M – H) $^-$]: 434.1746. Found: 434.1745.

2-(1-(6-Fluoro-8-(methylamino)-2-((2-methylpyrimidin-5-yl)-oxy)-9H-pyrimido[4,5-b]indol-4-yl)azetid-3-ylidene)propan-1-ol (34b). Compound **34b** (32 mg, 20% yield) was prepared from **11** (200 mg, 376 μmol), **32b** (139 mg, 931 μmol), K_2CO_3 (156 mg, 1.13 mmol), and TFA (2.0 mL, 26.9 mmol) in the same manner as described for **34a**. ^1H NMR (400 MHz, $\text{DMSO}-d_6$): δ 11.75 (s, 1H), 8.72 (s, 2H), 6.90 (d, $J = 10.4$ Hz, 1H), 6.30 (d, $J = 12.2$ Hz, 1H), 5.61 (s, 1H), 5.04 (s, 2H), 4.93 (s, 2H), 4.89–4.77 (m, 1H), 3.91 (s, 2H), 2.84 (d, $J = 4.7$ Hz, 3H), 2.67 (s, 3H), 1.56 (s, 3H). ^{13}C NMR (126 MHz, $\text{DMSO}-d_6$): δ 163.69, 161.90, 159.63, 158.81, 157.14, 151.13 (2C), 146.65, 136.96, 128.62, 122.48, 121.12, 118.94, 94.68, 94.36, 92.43, 62.70, 60.39, 59.85, 30.23, 25.44, 14.71. MS (ESI) m/z : 434.3 (M – H) $^-$. HRMS (ESI): Anal. Calcd for $\text{C}_{22}\text{H}_{21}\text{FN}_7\text{O}_2$ [(M – H) $^-$]: 434.1746. Found: 434.1739.

2-(1-(6-Fluoro-8-(methylamino)-2-((2-methylpyrimidin-5-yl)-oxy)-9H-pyrimido[4,5-b]indol-4-yl)azetid-3-ylidene)butan-1-ol (34c). Compound **34c** (44 mg, 31% yield) was prepared from **11** (170 mg, 317 μmol), **32c** (112 mg, 880 μmol), K_2CO_3 (132 mg, 958 μmol), and TFA (2.0 mL, 26.9 mmol) in the same manner as described for **34a**. ^1H NMR (500 MHz, $\text{DMSO}-d_6$): δ 11.69 (s, 1H), 8.72 (s, 2H), 6.91 (d, $J = 8.7$ Hz, 1H), 6.36–6.12 (m, 1H), 5.54 (d, $J = 4.2$ Hz, 1H), 5.02 (d, $J = 36.5$ Hz, 4H), 4.78 (t, $J = 5.6$ Hz, 1H), 3.97 (d, $J = 4.8$ Hz, 2H), 2.85 (d, $J = 4.8$ Hz, 3H), 2.67 (s, 3H), 2.00 (dd, $J = 14.6, 7.3$ Hz, 2H), 1.01 (t, $J = 7.6$ Hz, 3H). ^{13}C NMR (126 MHz, $\text{DMSO}-d_6$): δ 163.74, 161.94, 159.69, 158.83, 157.17, 151.18 (2C), 146.67, 136.96, 134.08, 122.53, 121.13, 118.97, 94.71, 94.44, 92.50, 60.75, 60.59, 59.78, 30.28, 25.46, 22.48, 12.77. MS (ESI) m/z : 448.3 (M – H) $^-$. HRMS (ESI): Anal. Calcd for $\text{C}_{23}\text{H}_{23}\text{FN}_7\text{O}_2$ [(M – H) $^-$]: 448.1903. Found: 448.1901.

2-(1-(6-Fluoro-8-(methylamino)-2-((2-methylpyrimidin-5-yl)-oxy)-9H-pyrimido[4,5-b]indol-4-yl)azetid-3-ylidene)-3-methylbutan-1-ol (34d). Compound **15** (250 mg, 568 μmol) and triethylamine (172 mg, 1.70 mmol) were dissolved in 5 mL of NMP. The BOP reagent (353 mg, 795 μmol) was added into the solution at 0 $^\circ\text{C}$ under an argon atmosphere and the reaction mixture was stirred for 30 min. Then, intermediate **32d** (146 mg, 1.04 mmol) dissolved in 5 mL of NMP was added dropwise to the mixture. The reaction mixture was heated to 50 $^\circ\text{C}$ and stirred for 1 h. The reaction mixture was poured into 15 mL of water and a white precipitate appeared. After filtration and drying, the white solid was redissolved in TFA (2.0 mL, 26.9 mmol). The reaction mixture was allowed to stir at room temperature for 2 min and then evaporated to dryness in vacuo. The residue was adjusted to pH ~8 by saturated solution of sodium bicarbonate. The mixture was extracted with ethyl acetate and the organic phase was washed with water and brine, dried over anhydrous sodium sulfate (Na_2SO_4), and filtered, and the filtrate was concentrated in vacuo. The residue was purified by chromatography on silica gel with DCM/methanol (10:1) to afford **34d** as a white solid (53 mg, 24% yield). ^1H NMR (600 MHz, $\text{DMSO}-d_6$): δ 11.66 (s, 1H), 8.69 (s, 2H), 6.86 (d, $J = 9.9$ Hz, 1H), 6.27 (d, $J = 10.6$ Hz, 1H), 5.50 (d, $J = 3.9$ Hz, 1H), 5.02 (d, $J = 38.3$ Hz, 4H), 4.69 (t, $J =$

5.5 Hz, 1H), 3.96 (d, $J = 4.3$ Hz, 2H), 2.82 (d, $J = 4.7$ Hz, 3H), 2.64 (s, 3H), 2.44–2.33 (m, 1H), 1.03 (s, 3H), 1.02 (s, 3H). ^{13}C NMR (151 MHz, $\text{DMSO}-d_6$): δ 163.74, 161.96, 159.61, 158.96, 157.14, 151.20 (2C), 146.66, 137.45, 136.95, 122.54, 121.11, 118.96, 94.65, 94.40, 92.47, 59.66, 56.49, 49.06, 30.27, 29.86, 25.46, 21.30 (2C). MS (ESI) m/z : 462.3 (M – H) $^-$. HRMS (ESI): Anal. Calcd for $\text{C}_{24}\text{H}_{25}\text{FN}_7\text{O}_2$ [(M – H) $^-$]: 462.2059. Found: 462.2051.

2-(1-(6-Fluoro-8-(methylamino)-2-(pyrazolo[1,5-*a*]pyrimidin-6-yl)oxy)-9H-pyrimido[4,5-*b*]indol-4-yl)azetid-3-ylidene)butan-1-ol (38). Compound **38** (18 mg, 32% yield) was prepared from **36** (70 mg, 120 μmol), **32c** (39 mg, 308 μmol), K_2CO_3 (49.82 mg, 360.48 μmol), and TFA (2.0 mL, 26.9 mmol) in the same manner as described for **34a**. ^1H NMR (500 MHz, $\text{DMSO}-d_6$): δ 11.69 (s, 1H), 9.37 (s, 1H), 8.70 (s, 1H), 8.25 (s, 1H), 6.91 (d, $J = 9.8$ Hz, 1H), 6.81 (s, 1H), 6.30 (d, $J = 11.8$ Hz, 1H), 5.48 (s, 1H), 5.06 (s, 2H), 4.99 (s, 2H), 4.77 (s, 1H), 3.96 (s, 2H), 2.84 (s, 3H), 1.99 (d, $J = 6.7$ Hz, 2H), 1.00 (t, $J = 7.1$ Hz, 3H). ^{13}C NMR (126 MHz, $\text{DMSO}-d_6$): δ 162.46, 159.71, 158.83, 157.18, 148.41, 146.41, 145.60, 138.46, 137.00, 134.10, 128.76, 122.52, 121.12, 118.97, 96.91, 94.69, 94.47, 92.52, 60.75, 60.58, 59.76, 30.28, 22.49, 12.76. MS (ESI) m/z : 475.4 (M + H) $^+$. HRMS (ESI): Anal. Calcd for $\text{C}_{24}\text{H}_{24}\text{FN}_8\text{O}_2$ [(M + H) $^+$]: 475.2001. Found: 475.2008.

4-(3-(1-Aminobutan-2-ylidene)azetid-1-yl)-6-fluoro-N-methyl-2-((2-methylpyrimidin-5-yl)thio)-9H-pyrimido[4,5-*b*]indol-8-amine (42a). Compound **42a** (62 mg, 61% yield) was prepared from **41a** (123 mg, 177 μmol), TFA (2.0 mL, 26.9 mmol), and 85% hydrazine hydrate (1.0 mL, 17.4 mmol) in the same manner as described for **26**. ^1H NMR (500 MHz, $\text{DMSO}-d_6$): δ 11.58 (s, 1H), 8.87 (s, 2H), 7.92 (s, 3H), 6.88 (dd, $J = 10.0, 1.7$ Hz, 1H), 6.30 (dd, $J = 12.1, 1.8$ Hz, 1H), 5.05 (s, 2H), 4.89 (s, 2H), 3.39 (d, $J = 5.3$ Hz, 2H), 2.82 (s, 3H), 2.69 (s, 3H), 2.09 (q, $J = 7.2$ Hz, 2H), 1.00 (t, $J = 7.5$ Hz, 3H). ^{13}C NMR (126 MHz, $\text{DMSO}-d_6$): δ 169.10, 165.22, 164.03 (2C), 162.19, 160.62–159.32, 157.36, 138.61, 132.06, 128.44, 125.44, 122.38, 120.01, 119.32, 116.98, 97.25, 95.93, 94.36, 61.41, 60.72, 39.76, 31.64, 27.35, 24.16, 13.77. MS (ESI) m/z : 465.3 (M + H) $^+$. HRMS (ESI): Anal. Calcd for $\text{C}_{23}\text{H}_{26}\text{FN}_8\text{S}$ [(M + H) $^+$]: 465.1980. Found: 465.1990.

4-(3-(1-Aminobutan-2-ylidene)azetid-1-yl)-2-((5-bromopyridin-2-yl)thio)-6-fluoro-N-methyl-9H-pyrimido[4,5-*b*]indol-8-amine (42b). Compound **42b** (33 mg, 57% yield) was prepared from **41b** (83 mg, 109 μmol), TFA (2.0 mL, 26.9 mmol), and 85% hydrazine hydrate (1.0 mL, 17.4 mmol) in the same manner as described for **26**. ^1H NMR (400 MHz, $\text{DMSO}-d_6$): δ 8.70 (s, 1H), 8.11 (s, 1H), 7.97 (s, 1H), 6.90 (s, 1H), 6.32 (s, 1H), 5.79 (s, 1H), 5.04 (s, 2H), 4.87 (s, 2H), 3.16 (s, 2H), 2.85 (s, 3H), 2.02 (s, 2H), 0.99 (s, 3H). ^{13}C NMR (126 MHz, $\text{DMSO}-d_6$): δ 163.36, 158.45, 155.85, 154.34, 150.67, 139.91, 137.22, 134.29, 131.19, 123.09, 121.04, 119.59, 118.78, 95.86, 94.54d, ($J = 23.3$ Hz), 92.88, 60.32, 59.62, 41.88, 30.22, 22.87, 12.71. MS (ESI) m/z : 528.2 (M + H) $^+$. HRMS (ESI): Anal. Calcd for $\text{C}_{23}\text{H}_{24}\text{BrFN}_7\text{S}$ [(M + H) $^+$]: 528.0976. Found: 528.0988.

6-Fluoro-4-(3-(1-hydroxybutan-2-ylidene)azetid-1-yl)-8-(methylamino)-N-(2-methylpyrimidin-5-yl)-9H-pyrimido[4,5-*b*]indole-2-carboxamide (47). Compound **46** (70 mg, 191 μmol) and triethylamine (57.85 mg, 572 μmol) were dissolved in 5 mL of NMP. The BOP reagent (101 mg, 229 μmol) was added into the solution at 0 $^\circ\text{C}$ under an argon atmosphere and the reaction mixture was stirred for 30 min. Then, intermediate **32c** (70 mg, 308 μmol) dissolved in 5 mL of NMP was added dropwise to the mixture. The reaction mixture was heated to 50 $^\circ\text{C}$ and stirred for 1 h. The reaction mixture was poured into 15 mL of water and a white precipitate appeared. The white crude product was obtained after filtration and dryness. It was purified by recrystallization in acetonitrile and methanol to afford compound **47** as a white solid. ^1H NMR (500 MHz, $\text{DMSO}-d_6$): δ 12.45 (s, 1H), 10.69 (s, 1H), 9.16 (s, 2H), 7.00 (d, $J = 9.5$ Hz, 1H), 6.76 (s, 1H), 6.37 (d, $J = 11.9$ Hz, 1H), 5.22 (s, 2H), 5.14 (s, 2H), 4.87 (s, 1H), 4.00 (s, 2H), 2.89 (d, $J = 3.2$ Hz, 3H), 2.64 (s, 3H), 2.05 (d, $J = 6.9$ Hz, 2H), 1.04 (t, $J = 7.1$ Hz, 3H). ^{13}C NMR (126 MHz, $\text{DMSO}-d_6$): δ 162.78, 162.18, 158.43, 157.93, 154.82, 152.88 (2C), 148.66, 137.24, 133.39, 131.23, 122.58, 122.31, 117.75, 97.94, 93.84, 92.58, 60.42, 60.12, 59.59, 29.50, 25.00, 21.98,

12.35. MS (ESI) m/z : 499.2 (M + Na)⁺. HRMS (ESI): Anal. Calcd for C₂₄H₂₅FN₈NaO₂ [(M + Na)⁺]: 499.1977. Found: 499.1975.

2-(1-(5,6-Difluoro-8-(methylamino)-2-((2-methylpyrimidin-5-yl)oxy)-9H-pyrimido[4,5-b]indol-4-yl)azetid-3-ylidene)butan-1-ol (**61**). Compound **61** (53 mg, 21% yield) was prepared from **53a** (300 mg, 545 μmol), **32c** (84 mg, 660 μmol), K₂CO₃ (225 mg, 1.63 mmol), and TFA (2.0 mL, 26.9 mmol) in the same manner as described for **34a**. ¹H NMR (500 MHz, DMSO-*d*₆): δ 11.82 (s, 1H), 8.70 (s, 2H), 6.73–6.52 (m, 1H), 6.39 (dd, *J* = 13.6, 6.7 Hz, 1H), 5.34 (d, *J* = 4.8 Hz, 1H), 4.47 (dd, *J* = 15.4, 4.3 Hz, 4H), 4.19 (d, *J* = 5.5 Hz, 2H), 2.81 (d, *J* = 4.9 Hz, 3H), 2.64 (s, 3H), 2.11 (q, *J* = 7.5 Hz, 2H), 0.92 (t, *J* = 7.6 Hz, 3H). ¹³C NMR (126 MHz, DMSO-*d*₆): δ 163.35, 162.64, 158.41, 157.39, 155.90, 150.73 (2C), 146.14, 135.98, 132.57, 132.49, 127.67, 120.27, 108.48, 92.73, 92.10, 76.82, 76.66, 35.03, 30.11, 24.95, 17.62, 12.74. MS (ESI) m/z : 468.3 (M + H)⁺. HRMS (ESI): Anal. Calcd for C₂₃H₂₄F₂N₇O₂ [(M + H)⁺]: 468.1954. Found: 468.1962.

4-(3-(1-Aminobutan-2-ylidene)azetid-1-yl)-5,6-difluoro-N-methyl-2-((2-methylpyrimidin-5-yl)oxy)-9H-pyrimido[4,5-b]indol-8-amine (**63a**). Compound **63a** (190 mg, 38% yield) was prepared from **53a** (300 mg, 545 μmol), **16k** (168 mg, 654 μmol), K₂CO₃ (225 mg, 1.63 mmol), TFA (2.0 mL, 26.9 mmol), and 85% hydrazine hydrate (1.0 mL, 17.4 mmol) in the same manner as described for **18k**. ¹H NMR (500 MHz, DMSO-*d*₆): δ 8.74 (s, 2H), 6.46 (dd, *J* = 13.4, 6.2 Hz, 1H), 5.47 (d, *J* = 4.5 Hz, 1H), 5.01 (s, 2H), 4.92 (s, 2H), 3.25 (s, 2H), 2.83 (d, *J* = 4.7 Hz, 3H), 2.68 (s, 3H), 2.07–2.01 (m, 2H), 0.98 (t, *J* = 7.5 Hz, 3H). ¹³C NMR (126 MHz, DMSO-*d*₆): δ 163.95, 161.86, 161.71, 158.29, 157.64, 151.20 (2C), 146.58, 132.59, 129.23, 127.82, 121.51, 118.96, 109.15, 93.52, 92.58, 60.94, 60.38, 60.22, 30.65, 25.47, 22.63, 12.51. MS (ESI) m/z : 467.2 (M + H)⁺. HRMS (ESI): Anal. Calcd for C₂₃H₂₅F₂N₈O [(M + H)⁺]: 467.2114. Found: 467.2104.

4-(3-(1-Aminobutan-2-ylidene)azetid-1-yl)-6-fluoro-N-(methyl-*d*₃)-2-((2-methylpyrimidin-5-yl)oxy)-9H-pyrimido[4,5-b]indol-8-amine (**63b**). Compound **63b** (70 mg, 33% yield) was prepared from **53b** (250 mg, 467 μmol), **16k** (215 mg, 840 μmol), K₂CO₃ (194 mg, 1.40 mmol), TFA (2.0 mL, 26.9 mmol), and 85% hydrazine hydrate (1.0 mL, 17.4 mmol) in the same manner as described for **18a**. ¹H NMR (500 MHz, DMSO-*d*₆): δ 8.72 (s, 2H), 6.91 (dd, *J* = 10.3, 2.2 Hz, 1H), 6.29 (dd, *J* = 12.1, 2.2 Hz, 1H), 5.53 (s, 1H), 5.08 (s, 2H), 4.94 (s, 2H), 3.16 (s, 2H), 2.67 (s, 3H), 2.03 (q, *J* = 7.5 Hz, 2H), 1.00 (t, *J* = 7.6 Hz, 3H). ¹³C NMR (126 MHz, DMSO-*d*₆): δ 163.72, 161.92, 159.65, 158.83, 157.15, 151.16 (2C), 146.66, 136.98, 134.85, 122.46, 121.14, 118.96, 94.70, 94.45, 92.46, 60.29, 59.66, 49.06, 42.04, 25.45, 22.84, 12.74. MS (ESI) m/z : 450.4 (M – H)[–]. HRMS (ESI): Anal. Calcd for C₂₃H₂₁D₃FN₈O [(M – H)[–]]: 450.2251. Found: 450.2244.

4-(3-(3-Aminobutan-2-ylidene)azetid-1-yl)-6-fluoro-N-(methyl-*d*₃)-2-((2-methylpyrimidin-5-yl)oxy)-9H-pyrimido[4,5-b]indol-8-amine (**63c**). Compound **63c** (78 mg, 37% yield) was prepared from **53b** (250 mg, 467 μmol), **16p** (215 mg, 840 μmol), K₂CO₃ (194 mg, 1.40 mmol), TFA (2.0 mL, 26.9 mmol), and 85% hydrazine hydrate (1.0 mL, 17.4 mmol) in the same manner as described for **18a**. ¹H NMR (500 MHz, DMSO-*d*₆): δ 8.72 (s, 2H), 6.91 (dd, *J* = 10.3, 2.1 Hz, 1H), 6.29 (dd, *J* = 12.0, 2.0 Hz, 1H), 5.56 (s, 1H), 5.06 (s, 2H), 4.87 (s, 2H), 3.54 (dd, *J* = 13.1, 6.5 Hz, 1H), 2.67 (s, 3H), 1.55 (s, 3H), 1.09 (d, *J* = 6.6 Hz, 3H). ¹³C NMR (126 MHz, DMSO-*d*₆): δ 163.21, 161.40, 159.14, 158.34, 156.65, 150.65 (2C), 146.16, 136.49, 132.15, 121.17, 120.65, 118.46, 94.21, 93.93, 91.95, 59.58, 59.21, 48.27, 26.31, 24.95, 21.01, 11.85. MS (ESI) m/z : 452.3 (M + H)⁺. HRMS (ESI): Anal. Calcd for C₂₃H₂₃D₃FN₈O [(M + H)⁺]: 452.2398. Found: 452.2398.

(*R*)-4-(3-(3-Aminobutan-2-ylidene)azetid-1-yl)-6-fluoro-N-(methyl-*d*₃)-2-((2-methylpyrimidin-5-yl)oxy)-9H-pyrimido[4,5-b]indol-8-amine (**63d**). Compound **63d** was prepared from **53b** (150 mg, 280 μmol), **16r** (101 mg, 392 μmol), K₂CO₃ (116 mg, 840 μmol), TFA (2.0 mL, 26.9 mmol), and 85% hydrazine hydrate (1.0 mL, 17.4 mmol) in the same manner as described for **18a**. It was redissolved in 5 mL of methanol and 5 mL of 4 M HCl methanol solution. After being stirred for 20 min, it was evaporated to dryness and the hydrochloride form of compound **63d** was obtained as a pale-

yellow solid (30 mg, 21% yield). ¹H NMR (500 MHz, DMSO-*d*₆): δ 11.99 (s, 1H), 8.74 (s, 2H), 8.31 (s, 3H), 7.00 (dd, *J* = 10.0, 1.7 Hz, 1H), 6.40 (dd, *J* = 11.8, 1.8 Hz, 1H), 5.15 (s, 2H), 4.91 (s, 2H), 3.95–3.83 (m, 1H), 2.68 (s, 3H), 1.67 (s, 3H), 1.31 (d, *J* = 6.7 Hz, 3H). ¹³C NMR (126 MHz, DMSO-*d*₆): δ 163.58, 161.73, 160.53, 159.65, 158.69, 157.24, 151.07 (2C), 146.65, 128.51, 125.46, 121.78, 119.21, 95.47, 94.75, 92.12, 59.87, 59.64, 47.66, 29.46, 25.34, 17.40, 12.20. MS (ESI) m/z : 452.2 (M + H)⁺. HRMS (ESI): Anal. Calcd for C₂₃H₂₃D₃FN₈O [(M + H)⁺]: 452.2396. Found: 452.2396. The ee value was 92.0%. Chiral HPLC retention time 29.28 min; column: CHIRALPAK IA column (250 mm × 4.6 mm, 5 μm); column temperature 30 °C; flow rate 0.5 mL/min; detection UV 254 nm; mobile phase: solvent A (80%) = methanol + 0.1% DEA, solvent B (20%) = ethanol + 0.1% DEA; total run time 40 min.

(*S*)-4-(3-(3-Aminobutan-2-ylidene)azetid-1-yl)-6-fluoro-N-(methyl-*d*₃)-2-((2-methylpyrimidin-5-yl)oxy)-9H-pyrimido[4,5-b]indol-8-amine (**63e**). Compound **63e** (33 mg, 23% yield) was prepared from **53b** (150 mg, 280 μmol), **62** (101 mg, 392 μmol), K₂CO₃ (116 mg, 840 μmol), TFA (2.0 mL, 26.9 mmol), and 85% hydrazine hydrate (1.0 mL, 17.4 mmol) in the same manner as described for **63d**. ¹H NMR (500 MHz, DMSO-*d*₆): δ 8.71 (s, 2H), 6.92 (dd, *J* = 10.3, 2.0 Hz, 1H), 6.29 (dd, *J* = 12.0, 2.0 Hz, 1H), 5.54 (s, 1H), 5.07 (s, 2H), 4.87 (s, 2H), 3.54 (dd, *J* = 13.0, 6.5 Hz, 1H), 2.67 (s, 3H), 1.55 (s, 3H), 1.09 (d, *J* = 6.6 Hz, 3H). ¹³C NMR (126 MHz, DMSO-*d*₆): δ 163.16, 161.36, 160.11, 159.12, 158.28, 156.60, 150.60 (2C), 146.10, 136.43, 132.01, 120.89, 118.40, 94.07, 93.78, 91.91, 59.54, 59.16, 48.20, 28.92, 24.90, 20.91, 11.80. MS (ESI) m/z : 452.2 (M + H)⁺. HRMS (ESI): Anal. Calcd for C₂₃H₂₃D₃FN₈O [(M + H)⁺]: 452.2396. Found: 452.2399. The ee value was 95.8%. Chiral HPLC retention time 23.41 min; column: CHIRALPAK IA column (250 mm × 4.6 mm, 5 μm); column temperature 30 °C; flow rate 0.5 mL/min; detection UV 254 nm; mobile phase: solvent A (80%) = methanol + 0.1% DEA, solvent B (20%) = ethanol + 0.1% DEA; total run time 40 min.

(*R*)-4-(3-(3-Aminobutan-2-ylidene)azetid-1-yl)-*N*-ethyl-6-fluoro-2-((2-methylpyrimidin-5-yl)oxy)-9H-pyrimido[4,5-b]indol-8-amine (**63f**). Compound **63f** (29 mg, 10% yield) was prepared from **53c** (360 mg, 659 μmol), **16r** (253 mg, 988 μmol), K₂CO₃ (273 mg, 1.98 mmol), TFA (2.0 mL, 26.9 mmol), and 85% hydrazine hydrate (1.0 mL, 17.4 mmol) in the same manner as described for **18a**. ¹H NMR (500 MHz, DMSO-*d*₆): δ 8.68 (d, *J* = 43.6 Hz, 2H), 6.91 (s, 1H), 6.32 (s, 1H), 5.52 (s, 1H), 5.08 (s, 2H), 4.88 (s, 2H), 3.60 (s, 3H), 2.67 (s, 3H), 1.57 (s, 3H), 1.24 (s, 3H), 1.12 (s, 3H). ¹³C NMR (126 MHz, DMSO-*d*₆): δ 163.71, 161.91, 160.60, 159.66, 158.78, 157.14, 151.16 (2C), 146.65, 135.91, 131.59, 122.68, 121.09, 94.61, 94.31, 92.74, 59.93, 59.66, 48.60, 38.04, 25.46, 20.92, 14.58, 12.33. MS (ESI) m/z : 463.2 (M + H)⁺. HRMS (ESI): Anal. Calcd for C₂₄H₂₈FN₈O [(M + H)⁺]: 463.2365. Found: 463.2371. The ee value was 95.2%. Chiral HPLC retention time 31.07 min; column: CHIRALPAK IA column (250 mm × 4.6 mm, 5 μm); column temperature 30 °C; flow rate 0.5 mL/min; detection UV 254 nm; mobile phase: solvent A (80%) = methanol + 0.1% DEA, solvent B (20%) = ethanol + 0.1% DEA; total run time 40 min.

1-(5-((3-(1-Aminobutan-2-ylidene)azetid-1-yl)-6-fluoro-8-((methyl-*d*₃)amino)-9H-pyrimido[4,5-b]indol-2-yl)oxy)pyrimidin-2-yl)ethan-1-ol (**65**). Compound **65** (65 mg, 24% yield) was prepared from **64** (340 mg, 573 μmol), **16k** (176 mg, 687 μmol), K₂CO₃ (237 mg, 1.72 mmol), TFA (2.0 mL, 26.9 mmol), and 85% hydrazine hydrate (1.0 mL, 17.4 mmol) in the same manner as described for **18a**. ¹H NMR (500 MHz, DMSO-*d*₆): δ 8.82 (s, 2H), 6.92 (d, *J* = 8.9 Hz, 1H), 6.30 (d, *J* = 10.9 Hz, 1H), 5.56 (s, 1H), 5.11 (s, 2H), 4.96 (s, 2H), 4.86 (q, *J* = 6.4 Hz, 1H), 3.19 (d, *J* = 18.1 Hz, 2H), 2.06 (dd, *J* = 14.1, 6.8 Hz, 2H), 1.47 (d, *J* = 6.5 Hz, 3H), 1.01 (t, *J* = 7.5 Hz, 3H). ¹³C NMR (126 MHz, DMSO-*d*₆): δ 167.86, 161.29, 159.09, 158.25, 156.47, 150.58 (2C), 146.58, 136.40, 132.66, 123.48, 120.56, 118.30, 94.13, 93.83, 91.88, 69.46, 59.65, 59.01, 40.65, 28.84, 22.64, 22.22, 12.05. MS (ESI) m/z : 482.3 (M + H)⁺. HRMS (ESI): Anal. Calcd for C₂₄H₂₃D₃FN₈O₂ [(M + H)⁺]: 482.2502. Found: 482.2513.

MIC Testing. The MICs of the target compounds against Gram-positive and Gram-negative bacteria were determined using

levofloxacin, meropenem (provided by Sichuan Primed Bio-Tech Group Co., Ltd.), GP-1 racemate, and cefiderocol (synthesized according to published procedures^{21,34}) as reference compounds. MIC values were determined using the broth microdilution protocol according to the methods of the Clinical and Laboratory Standards Institute (CLSI). All of the tested compounds except for levofloxacin and meropenem (dissolved in H₂O) were dissolved in DMSO to prepare a stock solution with a concentration of 64 $\mu\text{g}/\text{mL}$, and serial twofold dilutions were prepared from the stock solutions by the addition of culture broth to reach concentrations ranging from 64 to 0.008 $\mu\text{g}/\text{mL}$. The tested organisms were incubated in Mueller-Hinton broth medium at 35–37 °C for 18–20 h, and then, the MIC values were determined.

hERG K⁺ Channel Inhibition Assay. Whole-cell recordings were performed using automated QPatch (Sophion). The cells were voltage-clamped at a holding potential of –80 mV. The hERG current was activated by depolarizing at +20 mV for 5 s, after which the current was brought back to –50 mV and kept for 5 s to remove the inactivation and to observe the deactivating tail current. The maximum amount of tail current was used to determine hERG current amplitude. Compound stock solutions (10 or 30 mM in DMSO) were prepared before the experiments. The stock solutions were diluted to test concentrations upon use. After achieving a break-in (whole-cell) configuration, the cells were recorded for 120 s to assess current stability. The voltage protocol described above was then applied to the cells every 20 s throughout the procedure. Only stable cells with recording parameters above threshold were allowed for subsequent drug additions. External solution containing 0.1% DMSO (vehicle) was applied to the cells to establish the baseline. The current was allowed to stabilize for 3 min before the test compound was added. The cells were kept in the test solution until the compound's effect reached a steady state for a minimum of 3 min. Drug washout was performed with an external solution until the recovery of the current reached a steady state. Cisapride was used as the positive control. Data were analyzed using Assay software provided by Sophion, XLFit, or GraphPad Prism 6.0.

Molecular Docking. Small molecules were prepared using the LigPrep (version 2.4, Schrödinger, LLC, New York, NY, 2010). The protonation states of molecules were generated with Epik.³⁵ The crystal structure of GP-1 in complex with DNA Gyrase B (PDB id: 4KFG) was used for protein preparation and grid generation before docking. The docking procedure was performed using the Glide module of Maestro software (Glide, version 6; Schrödinger LLC, New York, NY, 2010) with the standard precision mode (SP). The binding interaction was analyzed and displayed by PyMOL (version 1.8).

Metabolic Stability Assay. The assay was performed using liver microsomes from rats and humans. The test compounds (final concentration of 0.1 μM in 0.01% DMSO with 0.005% bovine serum albumin) were incubated with live microsomes [0.33 mg/mL in 0.1 M tris(hydroxymethyl)-aminomethane/hydrochloric acid buffer (pH 7.4), cofactor MgCl₂ (5 mM), and reduced nicotinamide adenine dinucleotide phosphate (NADPH, 1 mM)] at 37 °C for 60 min. Aliquots were sampled at 0, 7, 17, 30, and 60 min, respectively, and methanol (cold in 4 °C) was added to terminate the reaction. After centrifugation (4000 rpm, 5 min), samples were then analyzed by liquid chromatography/tandem mass spectrometry (LC–MS/MS). The metabolic stability of the compounds is presented as the *in vitro* half-life ($T_{1/2}$), clearance (Cl_{int}), and metabolic bioavailability (MF %) in rat and human liver microsomes as previously described.^{36,37}

Metabolite Identification Assay. The assay was performed using liver microsomes from male SD rats. The test compound was preincubated in an incubation mixture consisted of 1 mg of microsomal protein/mL rat liver microsomes, 2 mM NADP, and 5 mM MgCl₂ in a total volume of 200 μL of potassium phosphate buffer (100 mM, pH 7.4) for 5 min at 37 °C. Aliquots were sampled at 0, 30, and 60 min, respectively, and 400 μL of cold acetonitrile (0.1% formic acid) was added to terminate the reaction. After centrifugation for 15 min at 16,000g, samples were then analyzed by UHPLC–MS/MS. Data are acquired using Xcalibur v4.1 software (Thermo Fisher Scientific) and processed using Xcalibur v4.1 software (Thermo

Fisher Scientific), Compound Discoverer 3.0 software (Thermo Fisher Scientific). The relative peak areas are determined from extracted ion chromatograms of liver microsome samples at 60 min.

Rat Pharmacokinetic Studies In Vivo. The pharmacokinetic parameters of compounds **18k**, **18m**, **18o**, **18p**, **31c**, and **61** were subjected to PK studies on male SD rats weighing between 180 and 280 g with three animals in each group. These tested compounds (5% DMSO + 5% EtOH + 40% PEG300 + 50% saline) were administered intravenously at a dose of 4 mg/kg. Serial specimens (0.3 mL) were collected via the retrobulbar vein 0.05, 0.25, 0.75, 2.0, 4.0, 8.0, and 24 h after administration and quantified by LC/MS/MS. The pharmacokinetic parameters of compounds **63c** (5 mg/kg), **63d** (5 mg/kg), **18r** (5 mg/kg), and **18r** (20 mg/kg) were subjected to PK studies on male SD rats weighing between 180 and 300 g with three animals in each group. These tested compounds (5% DMSO + 5% solutol + 90% saline) were administered intravenously. Serial specimens (0.2 mL) were collected via the retrobulbar vein 0.083, 0.25, 0.5, 1.0, 2.0, 4.0, 6.0, 8.0, and 24 h after administration and quantified by LC/MS/MS. Pharmacokinetic parameters were calculated from the mean plasma concentration by noncompartmental analysis. The protocol for this study was reviewed and approved by the Institutional Animal Care and Use Committee of the Shanghai Institute of Materia Medica, Chinese Academy of Sciences (Shanghai, China).

In Vivo Neutropenic Mouse Thigh Infection Experiments. Kunming mice (half male and half female) weighing between 18 and 22 g were used in this study with 8 mice in each administration group and 13 mice in the vehicle control group. The animals were housed at 20–25 °C and 40–70% relative humidity, with food and water available ad libitum throughout the study. The protocol for this study was reviewed and approved by the Institutional Animal Care and Use Committee of Sichuan Primed Bio-Tech Group Co., Ltd. Mice were rendered neutropenic (neutrophils, less than 100/mm³) by injection of cyclophosphamide intraperitoneally 4 days (150 mg/kg body weight) and 1 day (100 mg/kg) before thigh infection. Thigh infection in mice was carried out by intramuscular injection of 0.1 mL of inoculum of MDR *A. baumannii* clinical isolate into the right posterior thigh muscle (inoculum was prepared by inoculating single colony into fresh MHB media the day prior to thigh infection and cultured at 37 °C for 6 h. The overnight culture (the bacterial suspension) was further diluted to a concentration of 10⁷ cfu/mL in fresh MHB media prior to use. Two hours post thigh infection, compound **18r** was administered at a dose of 10, 20, and 30 mg/kg via intravenous tail injection, and levofloxacin in the positive control group was administered intravenously at a dose of 30 mg/kg. Two hours post thigh infection, the vehicle control group was administered intravenously equal volumes of saline, and 5 mice were sacrificed by euthanasia. The thigh muscles were removed for cfu determination as the data at 0 h. All other mice were sacrificed by euthanasia after 24 h of therapy, and the thigh muscles were removed. Thigh muscles were transferred into 1.5 mL sterile EP tubes and homogenized in 1 mL of saline for subsequent cfu determination.

Cellular Cytotoxicity Assay. HEK293 cells and L02 cells were plated in the 96-well plates at a density of 1 × 10⁴ cells per well for 48 h. Then, the cells were incubated with the test articles at different concentrations (1–200 μM) for another 48 h ($n = 6$). A Cell Counting Kit 8 (CCK 8) purchased from Yeasen Biotech Co., Ltd. (Shanghai, China) was used for the cytotoxicity assay with 10 μL of CCK 8 being added to each well for 2 h. The absorbance was measured using an automatic microplate reader (Biotek, Winooski, VT, USA) at a wavelength of 450 nm. The CC₅₀ values for each compound were calculated using GraphPad Prism 7.0 software (GraphPad Software Inc., La Jolla, CA, USA) and are shown as the mean value.

■ ASSOCIATED CONTENT

Supporting Information

The Supporting Information is available free of charge at <https://pubs.acs.org/doi/10.1021/acs.jmedchem.1c00621>.

More MIC data and details of tested compounds for Tables 1, 3, and 4; more MIC data and details of tested compounds for Table 5; metabolite identification of compound 18k in rat liver microsomes; proposed metabolic pathways of compound 18k; preparation and characterization data of all intermediates; NMR spectra and HRMS data of final compounds; and HPLC traces for lead compounds (PDF)

Molecular formula strings (CSV)

AUTHOR INFORMATION

Corresponding Author

Yushe Yang – State Key Laboratory of Drug Research, Shanghai Institute of Materia Medica, Chinese Academy of Sciences, Shanghai 201203, China; School of Pharmacy, University of Chinese Academy of Sciences, Beijing 100049, China; orcid.org/0000-0002-1007-2492; Phone: +86-21-50806786; Email: ysyang@mail.shcnc.ac.cn

Authors

Qidi Kong – State Key Laboratory of Drug Research, Shanghai Institute of Materia Medica, Chinese Academy of Sciences, Shanghai 201203, China; School of Pharmacy, University of Chinese Academy of Sciences, Beijing 100049, China

Wei Pan – State Key Laboratory of Drug Research, Shanghai Institute of Materia Medica, Chinese Academy of Sciences, Shanghai 201203, China

Heng Xu – School of Pharmaceutical Science and Technology, Hangzhou Institute for Advanced Study, University of Chinese Academy of Sciences, Hangzhou 310024, China

Yaru Xue – State Key Laboratory of Drug Research, Shanghai Institute of Materia Medica, Chinese Academy of Sciences, Shanghai 201203, China

Bin Guo – State Key Laboratory of Drug Research, Shanghai Institute of Materia Medica, Chinese Academy of Sciences, Shanghai 201203, China

Xin Meng – State Key Laboratory of Drug Research, Shanghai Institute of Materia Medica, Chinese Academy of Sciences, Shanghai 201203, China

Cheng Luo – State Key Laboratory of Drug Research, Shanghai Institute of Materia Medica, Chinese Academy of Sciences, Shanghai 201203, China; School of Pharmaceutical Science and Technology, Hangzhou Institute for Advanced Study, University of Chinese Academy of Sciences, Hangzhou 310024, China; orcid.org/0000-0003-3864-8382

Ting Wang – Department of Microbiology, Sichuan Primed Bio-Tech Group Company, Limited, Chengdu 610041, Sichuan Province, China

Shuhua Zhang – Department of Microbiology, Sichuan Primed Bio-Tech Group Company, Limited, Chengdu 610041, Sichuan Province, China

Complete contact information is available at:

<https://pubs.acs.org/10.1021/acs.jmedchem.1c00621>

Notes

The authors declare no competing financial interest.

ACKNOWLEDGMENTS

The authors thank financial support from the National Natural Science Foundation of China (no. 81872726).

ABBREVIATIONS

AMR, antimicrobial resistance; G⁺, Gram-positive; G⁻, Gram-negative; ESBLs, extended-spectrum β -lactamases; mCPBA, 3-chloroperoxybenzoic acid; Phth, phthaloyl; MeI, methyl iodide; PPh₃, triphenylphosphine; HATU, 2-(7-azabenzotriazol-1-yl)-N,N,N',N'-tetramethyluronium hexafluorophosphate; CS₂, carbon disulfide; DEA, diethylamine; MDR, multidrug-resistant; MSSA, methicillin-sensitive *Staphylococcus aureus*; MSSE, methicillin-sensitive *Staphylococcus epidermidis*; MRSE, methicillin-resistant *Staphylococcus epidermidis*; Eco, *Escherichia coli*; Kpn, *Klebsiella pneumoniae*; Aba, *Acinetobacter baumannii*; Pae, *Pseudomonas aeruginosa*; MF, metabolic bioavailability; SD, Sprague–Dawley; PK, pharmacokinetics; cfu, colony-forming units; PDB, Protein Data Bank

REFERENCES

- (1) Watkins, R. R.; Bonomo, R. A. Overview: Global and Local Impact of Antibiotic Resistance. *Infect. Dis. Clin. North Am.* **2016**, *30*, 313–322.
- (2) O'Neill, J.; Grande-Bretagne; Trust, W. Antimicrobial Resistance: Tackling a Crisis for the Health and Wealth of Nations. *Review on Antimicrobial Resistance*, 2014.
- (3) Shrivastava, R.; Chng, S.-S. Lipid Trafficking across the Gram-Negative Cell Envelope. *J. Biol. Chem.* **2019**, *294*, 14175–14184.
- (4) Li, X.-Z.; Plésiat, P.; Nikaido, H. The Challenge of Efflux-Mediated Antibiotic Resistance in Gram-Negative Bacteria. *Clin. Microbiol. Rev.* **2015**, *28*, 337–418.
- (5) Zgurskaya, H. I. An Old Problem in a New Light: Antibiotic Permeation Barriers. *ACS Infect. Dis.* **2020**, *6*, 3090–3091.
- (6) Kingwell, K. New Antibiotic Hits Gram-Negative Bacteria. *Nat. Rev. Drug Discovery* **2018**, *17*, 785.
- (7) Lewis, K. The Science of Antibiotic Discovery. *Cell* **2020**, *181*, 29–45.
- (8) Schillaci, D.; Spanò, V.; Parrino, B.; Carbone, A.; Montalbano, A.; Barraja, P.; Diana, P.; Cirrincione, G.; Cascioferro, S. Pharmaceutical Approaches to Target Antibiotic Resistance Mechanisms. *J. Med. Chem.* **2017**, *60*, 8268–8297.
- (9) Tacconelli, E.; Carrara, E.; Savoldi, A.; Harbarth, S.; Mendelson, M.; Monnet, D. L.; Pulcini, C.; Kahlmeter, G.; Kluytmans, J.; Carmeli, Y.; Ouellette, M.; Outterson, K.; Patel, J.; Cavalieri, M.; Cox, E. M.; Houchens, C. R.; Grayson, M. L.; Hansen, P.; Singh, N.; Theuretzbacher, U.; Magrini, N.; Aboderin, A. O.; Al-Abri, S. S.; Awang Jalil, N.; Benzoni, N.; Bhattacharya, S.; Brink, A. J.; Burkert, F. R.; Cars, O.; Cornaglia, G.; Dyr, O. J.; Friedrich, A. W.; Gales, A. C.; Gandra, S.; Giske, C. G.; Goff, D. A.; Goossens, H.; Gottlieb, T.; Guzman Blanco, M.; Hryniewicz, W.; Kattula, D.; Jinks, T.; Kanj, S. S.; Kerr, L.; Kieny, M.-P.; Kim, Y. S.; Kozlov, R. S.; Labarca, J.; Laxminarayan, R.; Leder, K.; Leibovici, L.; Levy-Hara, G.; Littman, J.; Malhotra-Kumar, S.; Manchanda, V.; Moja, L.; Ndoye, B.; Pan, A.; Paterson, D. L.; Paul, M.; Qiu, H.; Ramon-Pardo, P.; Rodríguez-Baño, J.; Sanguinetti, M.; Sengupta, S.; Sharland, M.; Si-Mehand, M.; Silver, L. L.; Song, W.; Steinbakk, M.; Thomsen, J.; Thwaites, G. E.; van der Meer, J. W.; Van Kinh, N.; Vega, S.; Villegas, M. V.; Wechsler-Fördös, A.; Wertheim, H. F. L.; Wesangula, E.; Woodford, N.; Yilmaz, F. O.; Zorzet, A. Discovery, Research, and Development of New Antibiotics: The Who Priority List of Antibiotic-Resistant Bacteria and Tuberculosis. *Lancet Infect. Dis.* **2018**, *18*, 318–327.
- (10) Hiasa, H. DNA Topoisomerases as Targets for Antibacterial Agents. In *DNA Topoisomerases: Methods and Protocols*; Drolet, M., Ed.; Springer New York: New York, NY, 2018; pp 47–62.
- (11) Mayer, C.; Janin, Y. L. Non-Quinolone Inhibitors of Bacterial Type Iia Topoisomerases: A Feat of Bioisosterism. *Chem. Rev.* **2014**, *114*, 2313–2342.
- (12) Laponogov, I.; Sohi, M. K.; Veselkov, D. A.; Pan, X.-S.; Sawhney, R.; Thompson, A. W.; McAuley, K. E.; Fisher, L. M.; Sanderson, M. R. Structural Insight into the Quinolone–DNA

Cleavage Complex of Type Iia Topoisomerases. *Nat. Struct. Mol. Biol.* **2009**, *16*, 667–669.

(13) Stokes, S. S.; Vemula, R.; Pucci, M. J. Advancement of Gyrb Inhibitors for Treatment of Infections Caused by Mycobacterium Tuberculosis and Non-Tuberculous Mycobacteria. *ACS Infect. Dis.* **2020**, *6*, 1323–1331.

(14) Bisacchi, G. S.; Manchester, J. I. A New-Class Antibacterial—Almost. Lessons in Drug Discovery and Development: A Critical Analysis of More Than 50 Years of Effort toward Atpase Inhibitors of DNA Gyrase and Topoisomerase Iv. *ACS Infect. Dis.* **2015**, *1*, 4–41.

(15) Skok, Ž.; Barančoková, M.; Benek, O.; Cruz, C. D.; Tammela, P.; Tomašič, T.; Zidar, N.; Mašič, L. P.; Zega, A.; Stevenson, C. E. M.; Mundy, J. E. A.; Lawson, D. M.; Maxwell, A.; Kikelj, D.; Ilaš, J. Exploring the Chemical Space of Benzothiazole-Based DNA Gyrase B Inhibitors. *ACS Med. Chem. Lett.* **2020**, *11*, 2433–2440.

(16) Dennie, J.; Vandell, A. G.; Inoue, S.; Gajee, R.; Pav, J.; Zhang, G.; Zamora, C.; Masuda, N.; Uchiyama, M.; Yamada, M.; Senaldi, G. A Phase I, Single-Ascending-Dose Study in Healthy Subjects to Assess the Safety, Tolerability, Pharmacokinetics, and Pharmacodynamics of Ds-2969b, a Novel Gyrb Inhibitor. *J. Clin. Pharmacol.* **2018**, *58*, 1557–1565.

(17) Vandell, A. G.; Inoue, S.; Dennie, J.; Nagasawa, Y.; Gajee, R.; Pav, J.; Zhang, G.; Zamora, C.; Masuda, N.; Senaldi, G. Phase 1 Study to Assess the Safety, Tolerability, Pharmacokinetics, and Pharmacodynamics of Multiple Oral Doses of Ds-2969b, a Novel Gyrb Inhibitor, in Healthy Subjects. *Antimicrob. Agents Chemother.* **2018**, *62*, No. e02537-17.

(18) Durcik, M.; Tomašič, T.; Zidar, N.; Zega, A.; Kikelj, D.; Mašič, L. P.; Ilaš, J. Atp-Competitive DNA Gyrase and Topoisomerase Iv Inhibitors as Antibacterial Agents. *Expert Opin. Ther. Pat.* **2019**, *29*, 171–180.

(19) Basarab, G. S.; Hill, P. J.; Garner, C. E.; Hull, K.; Green, O.; Sherer, B. A.; Dangel, P. B.; Manchester, J. L.; Bist, S.; Hauck, S.; Zhou, F.; Uria-Nickelsen, M.; Illingworth, R.; Alm, R.; Rooney, M.; Eakin, A. E. Optimization of Pyrrolamide Topoisomerase Ii Inhibitors toward Identification of an Antibacterial Clinical Candidate (Azd5099). *J. Med. Chem.* **2014**, *57*, 6060–6082.

(20) Tari, L. W.; Li, X.; Trzoss, M.; Bensen, D. C.; Chen, Z.; Lam, T.; Zhang, J.; Lee, S. J.; Hough, G.; Phillipson, D.; Akers-Rodriguez, S.; Cunningham, M. L.; Kwan, B. P.; Nelson, K. J.; Castellano, A.; Locke, J. B.; Brown-Driver, V.; Murphy, T. M.; Ong, V. S.; Pillar, C. M.; Shinabarger, D. L.; Nix, J.; Lightstone, F. C.; Wong, S. E.; Nguyen, T. B.; Shaw, K. J.; Finn, J. Tricyclic Gyrb/Pare (Tribe) Inhibitors: A New Class of Broad-Spectrum Dual-Targeting Antibacterial Agents. *PLoS One* **2013**, *8*, No. e84409.

(21) Finn, J.; Tari, L. W.; Chen, Z.; Zhang, J.; Phillipson, D.; Lee, S. J.; Trzoss, M.; Bensen, D.; Li, X.; Teng, M.; Ong, V.; Borchardt, A. J.; Lam, T. T. Tricyclic Gyrase Inhibitors. WO 2015038661 A1, 2015.

(22) Dey, F.; Hu, Y.; Liu, Y.; Lin, X.; Shen, H.; Shi, H.; Tan, X.; Vercruysse, M.; Yan, S.; Zhou, C.; Zhou, M. Novel Pyrido[2,3-B]Indole Compounds for the Treatment and Prophylaxis of Bacterial Infection. WO 2018178041 A1, 2018.

(23) Hu, Y.; Shi, H.; Zhou, M.; Ren, Q.; Zhu, W.; Zhang, W.; Zhang, Z.; Zhou, C.; Liu, Y.; Ding, X.; Shen, H. C.; Yan, S. F.; Dey, F.; Wu, W.; Zhai, G.; Zhou, Z.; Xu, Z.; Ji, Y.; Lv, H.; Jiang, T.; Wang, W.; Xu, Y.; Vercruysse, M.; Yao, X.; Mao, Y.; Yu, X.; Bradley, K.; Tan, X. Discovery of Pyrido[2,3-B]Indole Derivatives with Gram-Negative Activity Targeting Both DNA Gyrase and Topoisomerase Iv. *J. Med. Chem.* **2020**, *63*, 9623–9649.

(24) Ho, S. Y.; Wang, W.; Ng, F. M.; Wong, Y. X.; Poh, Z. Y.; Tan, S. W. E.; Ang, S. H.; Liew, S. S.; Joyner Wong, Y. S.; Tan, Y.; Poulsen, A.; Pendharkar, V.; Sangthongpitag, K.; Manchester, J.; Basarab, G.; Hill, J.; Keller, T. H.; Cherian, J. Discovery of Dual Gyrb/Pare Inhibitors Active against Gram-Negative Bacteria. *Eur. J. Med. Chem.* **2018**, *157*, 610–621.

(25) Richter, M. F.; Drown, B. S.; Riley, A. P.; Garcia, A.; Shirai, T.; Svec, R. L.; Hergenrother, P. J. Predictive Compound Accumulation Rules Yield a Broad-Spectrum Antibiotic. *Nature* **2017**, *545*, 299–304.

(26) Keating, T. A.; Lister, T.; Verheijen, J. C. New Antibacterial Agents: Patent Applications Published in 2011. *Pharm. Pat. Anal.* **2014**, *3*, 87–112.

(27) Gjorgjieva, M.; Tomašič, T.; Barančokova, M.; Katsamakas, S.; Ilaš, J.; Tammela, P.; Peterlin Mašič, L.; Kikelj, D. Discovery of Benzothiazole Scaffold-Based DNA Gyrase B Inhibitors. *J. Med. Chem.* **2016**, *59*, 8941–8954.

(28) Tiz, D. B.; Skok, Ž.; Durcik, M.; Tomašič, T.; Mašič, L. P.; Ilaš, J.; Zega, A.; Draskovits, G.; Révész, T.; Nyerges, Á.; Pál, C.; Cruz, C. D.; Tammela, P.; Žigon, D.; Kikelj, D.; Zidar, N. An Optimised Series of Substituted N-Phenylpyrrolamides as DNA Gyrase B Inhibitors. *Eur. J. Med. Chem.* **2019**, *167*, 269–290.

(29) Bensen, D.; Chen, Z.; Finn, J.; Lam, T. T.; Lee, S. J.; Li, X.; Phillipson, D. W.; Tari, L. W.; Trzoss, M.; Zhang, J. Tricyclic Gyrase Inhibitors. U.S. Patent 9,732,083 B2, 2017.

(30) Grant, E. B.; Macielag, M. J.; Xu, X.; Paget, S. D.; Weidner-Wells, M. A. 7-Amino Alkylidene-Heterocyclic Quinolones and Naphthyridones. WO 2005033108 A1, 2005.

(31) McGarry, D. H.; Cooper, I. R.; Walker, R.; Warrilow, C. E.; Pichowicz, M.; Ratcliffe, A. J.; Salisbury, A.-M.; Savage, V. J.; Moyo, E.; Maclean, J.; Smith, A.; Charrier, C.; Stokes, N. R.; Lindsay, D. M.; Kerr, W. J. Design, Synthesis and Antibacterial Properties of Pyrimido[4,5-B]Indol-8-Amine Inhibitors of DNA Gyrase. *Bioorg. Med. Chem. Lett.* **2018**, *28*, 2998–3003.

(32) Gant, T. G. Using Deuterium in Drug Discovery: Leaving the Label in the Drug. *J. Med. Chem.* **2014**, *57*, 3595–3611.

(33) Kong, Q.; Yang, Y. Recent Advances in Antibacterial Agents. *Bioorg. Med. Chem. Lett.* **2021**, *35*, 127799.

(34) Aoki, T.; Yoshizawa, H.; Yamawaki, K.; Yokoo, K.; Sato, J.; Hisakawa, S.; Hasegawa, Y.; Kusano, H.; Sano, M.; Sugimoto, H.; Nishitani, Y.; Sato, T.; Tsuji, M.; Nakamura, R.; Nishikawa, T.; Yamano, Y. Cefiderocol (S-649266), a New Siderophore Cephalosporin Exhibiting Potent Activities against *Pseudomonas Aeruginosa* and Other Gram-Negative Pathogens Including Multi-Drug Resistant Bacteria: Structure Activity Relationship. *Eur. J. Med. Chem.* **2018**, *155*, 847–868.

(35) Shelley, J. C.; Cholleti, A.; Frye, L. L.; Greenwood, J. R.; Timlin, M. R.; Uchimaya, M. Epik: a software program for pK_a prediction and protonation state generation for drug-like molecules. *J. Comput.-Aided Mol. Des.* **2007**, *21*, 681–691.

(36) Obach, R. S. Prediction of Human Clearance of Twenty-Nine Drugs from Hepatic Microsomal Intrinsic Clearance Data: An Examination of in Vitro Half-Life Approach and Nonspecific Binding to Microsomes. *Drug Metab. Dispos.* **1999**, *27*, 1350.

(37) Lau, Y. Y.; Krishna, G.; Yumibe, N. P.; Grotz, D. E.; Sapidou, E.; Norton, L.; Chu, I.; Chen, C.; Soares, A. D.; Lin, C. C. The Use of in Vitro Metabolic Stability for Rapid Selection of Compounds in Early Discovery Based on Their Expected Hepatic Extraction Ratios. *Pharm. Res.* **2002**, *19*, 1606–1610.